On internal resonances in pipes conveying pulsating fluid for beam, stretched-beam, and string models

Köroğlu, Ege; van Horssen, Wim T.

DOI
10.1007/s11071-024-10778-6

Publication date
2025

Document Version
Final published version

Published in
Nonlinear Dynamics

Citation (APA)
Köroğlu, E., & van Horssen, W. T. (2025). On internal resonances in pipes conveying pulsating fluid for beam, stretched-beam, and string models. *Nonlinear Dynamics*, *113*(22), 30731-30768. https://doi.org/10.1007/s11071-024-10778-6

Nonlinear Dyn
https://doi.org/10.1007/s11071-024-10778-6

RESEARCH

On internal resonances in pipes conveying pulsating fluid for beam, stretched-beam, and string models

Ege Köroğlu · Wim T. van Horssen

Received: 28 June 2024 / Accepted: 9 December 2024

Abstract In this paper, we investigate an initial-boundary value problem for a linear Euler-Bernoulli beam equation governing the dynamics of pipes conveying fluid. The fluid flow velocity inside the pipe is assumed to have a small amplitude and to be time-varying, that is, $V(t) = \varepsilon(V_0 + V_1 \sin(\Omega t))$, where a two time-scales perturbation method is applied to construct approximations of the solutions. We explore fluid velocity pulsation frequencies Ω that lead to resonance in the pipe system. Depending on the order of bending stiffness, we study beam, stretched-beam and string models, each displaying distinct resonance behaviour. For special values of the frequency Ω and the bending stiffness, resonance frequencies can coincide, leading to internal resonances that exhibit more complex dynamical behaviour. We investigate both pure and detuned internal resonance scenarios, highlighting how early truncation in the number of oscillation modes leads to erroneous approximations and incorrect stability conclusions.

Keywords Pipes conveying fluid · Transversal vibration · Parametric resonance · Internal resonance · Two time-scales perturbation method · Stability analysis

E. Köroğlu (✉) · W. T. van Horssen
Department of Applied Mathematics, Delft University of Technology, Mekelweg 4, Delft 2628, CD, The Netherlands
e-mail: e.koroglu@tudelft.nl

W. T. van Horssen
e-mail: w.t.vanhorssen@tudelft.nl

1 Introduction

In numerous industries and infrastructures, pipe structures are essential for operations requiring the transportation of fluid. Including urban water distribution, the extraction and transportation of oil and gas in refineries and offshore platforms, and fuel supply mechanisms in engine systems, pipes play a crucial role in many industrial applications. However, due to the type of pump being used, such as reciprocating pumps, or due to the instabilities of the fluid flow, velocity inside the pipe may demonstrate periodic time variations. The fluctuations of the fluid velocity can lead to oscillations in the pipe structures, which may present potential challenges to the integrity, safety and longevity of the pipe structure.

The first known written study in the field of pipes conveying fluid belongs to Bourrières [1], who examined in 1939 both string-like and beam-like cases. The studies on this subject were re-initiated by Ashley and Haviland [2], being unaware of the previous works. They modelled the pipe as a beam-like structure and studied the dynamics of a simply supported pipe and travelling waves in an infinite pipe. The model for simply supported pipes was later improved by Housner [3]. Benjamin [4] was the first to apply Hamilton's principle, in his study of articulated cantilevered pipes. The first complete derivation for the linear equation of motion for time-dependent fluid velocity was developed in 1974 by Païdoussis and Issid [5], employing both Newtonian and Lagrangian mechanics. Two years

Published online: 20 January 2025

later, by considering the shear deformations, Païdoussis and Laithier [6] were the first ones to obtain a Timoshenko beam model for pipes conveying fluid. Semler et al. [7] derived the nonlinear system of partial differential equations governing the dynamics of pipes conveying fluid, considering the effects of longitudinal deflections and higher-order curvature terms for strain expression.

The first known research on pipes conveying pulsating fluid belongs to Chen [8], where he considered the fluid velocity inside a simply supported pipe to exhibit a periodic time variation around a mean value. Employing the Galerkin truncation method, a set of Mathieu-Hill-type equations were obtained, and the parametric and combination resonances were investigated. Païdoussis and Issid [5] improved the derivation of linear equations of motion considering axial deflections and studied these equations using a two-term truncation. Studies of parametric and combination resonances have covered various pipe configurations, including articulated (Bohn and Herrmann [9]), cantilevered and clamped-clamped (Païdoussis and Sundararajan [10]), as well as simply supported and clamped-clamped arrangements (Ariaratnam and Sri Namachchivaya [11]). In terms of nonlinear equations of motions, Sri Namachchivaya [12], Sri Namachchivaya and Tien [13], Semler and Païdoussis [14], Öz and Boyaci [15] made significant contributions to the literature of nonlinear equations of motion governing pipes conveying pulsatile fluids, investigating various parametric resonances. Jin and Song [16] observed overlap of different resonances, and Panda and Kar [17,18] studied cases of resonance overlap in nonlinear equations of motion. External flow-induced vibrations have been studied for strings by Luongo et al. [19], Di Nino and Luongo [20], while Wang et al. [21] focused on pipes modelled as beams. These studies commonly assumed that a small number of vibration modes are responsible for the dynamics of the infinite-dimensional pipe systems. Therefore, the predominant "analytical" method of solution in this field has been the Galerkin truncation method, which remains the most popular method. It has also been used extensively for studying parametric and internal resonances in pipes conveying fluids and is employed in most recent papers [22–29].

The problems of pipes conveying fluid are closely related to the problems of axially moving continua, such as conveyor belts. Equations of both problems have significant mathematical similarities. In their study of conveyor belts with negligible bending stiffness, using a multiple time scales method, Suweken and van Horssen [30] have shown that for string-like conveyor belt problems, infinitely many modes interact with each other for certain velocity fluctuation frequencies. Hence, it was shown that the truncation method was inapplicable. In their further study, Suweken and van Horssen [31] investigated the beam-like equations for conveyor belt problems assuming that the bending stiffness is non-negligible. They studied combination resonances and internal resonances assuming that the belt velocity has a periodic time variation with a small average amplitude. They discovered that three-mode of sum and difference type resonances may overlap for certain parameter values, leading up to three-mode or four-mode interactions, and they studied three-mode interactions in detail. In their next paper, Suweken and van Horssen [32] considered cubic nonlinearities in their beam-like model and studied these internal resonances and changes in the stability of the nonlinear system. Pakdemirli and Öz [33] studied a linear problem using infinite dimensional eigenfunction expansion and reported matching resonance frequencies as in the study [31] for vanishing average fluid velocity. General expressions for eigenfunctions are obtained for infinite dimensional systems in [33]. For extending the natural frequencies to vanishing average fluid velocity, non-existing principle resonances, combination resonances and $\Omega = 0$ resonances are reported. This is due to the fact that the general form of eigenfunctions obtained does not explicitly provide orthogonality conditions that give restrictions on resonant mode numbers.

In 2003, while working on an axially moving continuum with small bending stiffness, van Horssen [34] introduced a new solution using the Laplace transform, providing an exact solution of the non-self-adjoint problem for the string-like problem. Van Horssen and Ponomareva [35], presented the superiority of this Laplace transform approach to the more popular finite dimensional eigenfunction expansion. A further study from Ponomareva and van Horssen [36] on axially moving strings with periodically time-varying velocity, employing the Laplace transform and multiple time scales methods, showed the inapplicability of the truncation method due to the interaction of infinitely many modes. This interaction leads to the neglect of energy contributions from higher modes when the system is truncated. Malookani and van Horssen [37,38], Sandilo

and van Horssen [39] have shown that the truncation method leads to incorrect stability conclusions for the infinite dimensional systems. Malookani and van Horssen [40,41] solved the infinite-dimensional problem for special initial conditions using the method of characteristic coordinates.

Andrianov and van Horssen [42], and Ponomareva and van Horssen [43] studied the transition from string to beam behaviour for an axially moving continuum with harmonic time variations and small average velocity. Their studies revealed for lower vibration modes that the terms associated with bending stiffness can be neglected, resulting in a string-like equation. Conversely, at higher frequencies, the contribution of the bending stiffness terms becomes significant, leading to a string-beam or even a beam model.

In this paper, we aim to link advancements in the study of accelerating continua to pipes conveying pulsating fluid. We study the dynamics of pipes with small average fluid velocity, using multiple-time scales perturbation approximations for the infinite-dimensional problem. With this approach, beam-like, stretched beam-like and string-like models occurring as a result of varying orders of bending stiffness are studied. We provide a detailed study of potential resonant cases and internal resonances for each model. Several analytical findings are validated through numerical studies using finite difference methods (FDM). Additionally, we discuss the possible complications that may arise from using the truncation method. For certain fluid pulsation frequencies, we show that applying the Galerkin truncation method results in incorrect approximations of the solutions for the infinite-dimensional system.

The structure of this paper is as follows. In Sect. 2, the derivation of the equation of motion is briefly given. The non-dimensional equations of motion are derived, and the problem is defined. In Sect. 3, the two-time-scale perturbation method is applied to the problem. In Sect. 4, the fluid velocity pulsation frequencies leading to resonance are determined. In Sect. 5, the concept of transition across models is presented with respect to varying orders of bending stiffness. In Sect. 6, resonance coincidence scenarios are investigated for each model. In Sect. 7, numerical investigations are presented. In Sect. 8, conclusions are drawn, and remarks are made.

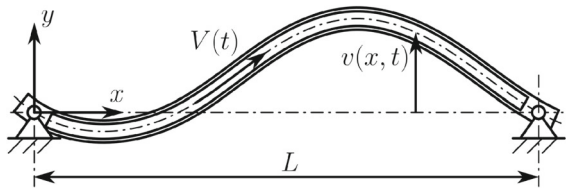

Fig. 1 Schematic diagram of the simply supported pipe system

2 Model

2.1 Derivation of equation of motions

A horizontally placed pipe of length L is assumed to be simply supported at both ends. The transverse displacement of the pipe's natural axis (in $y-$direction) at axial coordinate x and at time t is denoted by $v(x,t)$. The fluid flow velocity inside the pipe is denoted by $V(t)$. The pipe is assumed to have uniform material properties and cross-section S. The mass per unit length of the pipe and the fluid are given as m and M, respectively, with gravitational acceleration g, axial tension P, Young's modulus E, viscoelastic damping coefficient η, and area moment of inertia I. The schematic diagram of the pipe structure is shown in Fig. 1.

In this study, Hamilton's principle will be used to derive the linear equations of motion. The pipe structure is modeled as an Euler-Bernoulli beam, thus the shear deformations are neglected. Hamilton's principle for deformable bodies is expressed as:

$$\delta \int_{t_1}^{t_2} \mathcal{L} dt + \int_{t_1}^{t_2} \delta \mathcal{W} dt = 0, \tag{1}$$

where $\mathcal{L}$ is the Lagrangian, defined as $\mathcal{L} = \mathcal{T} - \mathcal{V}$; $\mathcal{T}$ and $\mathcal{V}$ represent the kinetic an potential energies, respectively, and $\mathcal{W}$ is the virtual work done by non-conservative forces. δ is the variation of a function.

The total kinetic energy of the pipe system, denoted by $\mathcal{T}$, consists of contributions from both the pipe $\mathcal{T}_p$ and fluid $\mathcal{T}_f$, expressed as $\mathcal{T} = \mathcal{T}_p + \mathcal{T}_f$. These components are defined as:

$$\begin{aligned} \mathcal{T}_p &= \frac{1}{2} m \int_0^L v_t^2 dx, \\ \mathcal{T}_f &= \frac{1}{2} M \int_0^L \left(V^2 + v_t^2 + 2V v_x v_t + V^2 v_x^2 \right) dx, \end{aligned} \tag{2}$$

where v_t and v_x are time and space derivatives of v, respectively. The derivation of $\mathcal{T}_f$ is well described in [5].

Similarly, the potential energy of the system, $\mathcal{V}$, consists of the contributions from both the pipe $\mathcal{V}_p$ and fluid $\mathcal{V}_f$, and is given by $\mathcal{V} = \mathcal{V}_p + \mathcal{V}_f$. Due to the effects of bending resistance, axial tension and gravity, the potential energy of pipe and fluid can be expressed as:

$$\begin{aligned} \mathcal{V}_p &= \int_0^L \left(\frac{1}{2}EI(v_{xx})^2 + \frac{1}{2}Pv_x^2 + mgv\right)dx, \\ \mathcal{V}_f &= Mg\int_0^L v dx. \end{aligned} \tag{3}$$

In this study, we assume that the pipe structure exhibits Kelvin-Voigt viscoelastic damping characteristics. This assumption corresponds to the $\sigma = E\epsilon + \eta\frac{d\epsilon}{dt}$ stress-strain relation, where σ and ϵ denote strain and stress respectively. The energy contribution of the linear elastic component of this expression is treated in (3). The contribution of Kelvin-Voigt viscoelastic damping on stress is given by $\sigma_{\mathrm{KV}} := \eta\frac{d\epsilon}{dt} = \eta y v_{txx}$.

Considering the cross-section of the pipe, denoted by S, the variation of virtual work of non-conservative forces is expressed as:

$$\begin{aligned} \delta\mathcal{W}_{\mathrm{KV}} &= -\int_0^L \int_S (\sigma_{\mathrm{KV}}\delta\epsilon) dS dx \\ &= -\int_0^L \int_S (\eta y v_{txx}\delta(y v_{xx})) dS dx \\ &= -\int_0^L (\eta I v_{txx}\delta v_{xx}) dx. \end{aligned} \tag{4}$$

Applying δ to the Lagrangian in (1) and considering the virtual work, the non-autonomous equation of motion can be derived as:

$$\begin{aligned} &\eta I v_{txxxx} + EIv_{xxxx} + (MV^2 - P)v_{xx} + 2MVv_{xt} \\ &\quad + (m+M)v_{tt} + MV_t v_x + (m+M)g = 0, \end{aligned} \tag{5}$$

with the natural boundary conditions

at $x = 0$

$$\begin{cases} MV(v_t + Vv_x) + Pv_x + EIv_{xxx} + \eta v_{txxx} = 0, \\ EIv_{xx} + \eta I v_{txx} = 0, \end{cases}$$

and at $x = 1$

$$\begin{cases} MV(v_t + Vv_x) + Pv_x + EIv_{xxx} + \eta v_{txxx} = 0, \\ EIv_{xx} + \eta I v_{txx} = 0. \end{cases} \tag{6}$$

2.2 Non-dimensionalization

To apply non-dimensionalization, we chose the characteristic values for the variables: $x_c = v_c = L$ and $t_c = \sqrt{\frac{m+M}{P}}L$. We then introduce the dimensionless parameters as follows:

$$\begin{aligned} &x^* = \frac{x}{L}, \quad v^* = \frac{v}{L}, \quad t^* = \sqrt{\frac{P}{m+M}}\frac{t}{L}, \\ &\alpha = \frac{\eta I}{\varepsilon L^3\sqrt{(m+M)P}}, \quad V^* = \sqrt{\frac{M}{P}}V, \\ &\mu = \frac{EI}{PL^2}, \quad \beta = \frac{M}{m+M}, \quad \gamma = \frac{m+M}{P}Lg. \end{aligned} \tag{7}$$

Here, the dimensionless parameter ε indicates that the viscoelastic damping coefficient η is small. By substituting the dimensionless parameters as defined above into the governing Eq. (5), we obtain the dimensionless form:

$$\begin{aligned} &\varepsilon\alpha v_{txxxx} + \mu v_{xxxx} + (V^2 - 1)v_{xx} \\ &\quad + 2\sqrt{\beta}Vv_{xt} + v_{tt} + \sqrt{\beta}V_t v_x + \gamma = 0. \end{aligned} \tag{8}$$

2.3 Problem definition

In this study, the fluid velocity inside the pipe is assumed to have a small amplitude with harmonic time variation, expressed as $V(t) = \varepsilon(V_0 + V_1\sin(\Omega t))$, where $V_0 > |V_1|$ and $0 < \varepsilon \ll 1$. With this choice, both the viscoelastic damping and fluid velocity are of $\mathcal{O}(\varepsilon)$. However, this choice does not exclude the possibility that η may be much smaller than $V(t)$. The dimensionless non-autonomous partial differential equation that governs the transversal motion of a simply supported

horizontal pipe is given by:

$$\begin{aligned}&\varepsilon\alpha v_{txxxx} + \mu v_{xxxx}\\&\quad + (\varepsilon^2(V_0 + V_1\sin(\Omega t))^2 - 1)v_{xx}\\&\quad + 2\varepsilon\sqrt{\beta}(V_0 + V_1\sin(\Omega t))v_{xt} + v_{tt}\\&\quad + \varepsilon\sqrt{\beta}V_1\Omega\cos(\Omega t)v_x + \gamma = 0,\end{aligned} \tag{9}$$

for $0 < x < 1$ and $t > 0$, with the boundary conditions:

$$\begin{aligned}&v(0,t) = v_{xx}(0,t) = 0,\\&v(1,t) = v_{xx}(1,t) = 0,\end{aligned} \tag{10}$$

for $t > 0$, and the initial conditions:

$$\begin{aligned}&v(x,0) = \phi(x),\\&v_t(x,0) = \psi(x),\end{aligned} \tag{11}$$

for $0 < x < 1$. The initial conditions $v(x,0) = \phi(x)$ and $v_t(x,0) = \psi(x)$ are necessary for the well-posedness of the problem. Although this study does not focus on the existence and uniqueness of solutions, these initial conditions are crucial for setting the initial energy distribution across modes, which is essential for the stability analysis.

3 Methods

3.1 Formal asymptotic approximations

It can be observed that Eq. (9) contains a constant non-homogeneous term, γ. Hence we propose a solution in the form:

$$v(x,t) = v_s(x) + v_0(x,t) + \varepsilon v_1(x,t) + \mathcal{O}(\varepsilon^2), \tag{12}$$

where $v_s(x)$ is the static solution, and solves the boundary value problem

$$\begin{aligned}&\mu v_s'''' - v_s'' + \gamma = 0,\\&v_s(0) = v_s(1) = v_s''(0) = v_s''(1) = 0,\end{aligned} \tag{13}$$

for $0 < x < 1$, and ε is a small parameter. The homogeneous $\mathcal{O}(1)$ problem is:

$$\begin{aligned}&\mu\frac{\partial^4 v_0}{\partial x^4} - \frac{\partial^2 v_0}{\partial x^2} + \frac{\partial^2 v_0}{\partial t^2} = 0,\\&\text{BC's: } v_0(0,t) = \tfrac{\partial^2 v_0}{\partial x^2}(0,t) = 0,\\&\qquad v_0(1,t) = \tfrac{\partial^2 v_0}{\partial x^2}(1,t) = 0,\\&\text{IC's: } v_0(x,0) = \phi(x) - v_s(x),\\&\qquad \tfrac{\partial v_0}{\partial t}(x,0) = \psi(x),\end{aligned} \tag{14}$$

and the $\mathcal{O}(\varepsilon)$ problem is:

$$\begin{aligned}&\mu\frac{\partial^4 v_1}{\partial x^4} - \frac{\partial^2 v_1}{\partial x^2} + \frac{\partial^2 v_1}{\partial t^2}\\&\quad = -\alpha\frac{\partial^5 v_0}{\partial x^4\partial t} - \sqrt{\beta}V_1\Omega\cos(\Omega t_0)\frac{\partial v_0}{\partial x}\\&\qquad - 2\sqrt{\beta}(V_0 + V_1\sin(\Omega t_0))\frac{\partial^2 v_0}{\partial x\partial t},\\&\text{BC's: } v_1(0,t) = \frac{\partial^2 v_1}{\partial x^2}(0,t) = 0,\\&\qquad v_1(1,t) = \frac{\partial^2 v_1}{\partial x^2}(1,t) = 0,\\&\text{IC's: } v_1(x,0) = 0, \quad \frac{\partial v_1}{\partial t}(x,0) = 0.\end{aligned} \tag{15}$$

By solving problem (13), as detailed in Appendix A, we obtain the static solution given by:

$$\begin{aligned}v_s(x) = &-\gamma\mu\,\mathrm{sech}\left(\frac{1}{2\sqrt{\mu}}\right)\cosh\left(\frac{1-2x}{2\sqrt{\mu}}\right)\\&+ \frac{\gamma}{2}(x^2 - x + 2\mu).\end{aligned} \tag{16}$$

Assuming that a solution of Eq. (14) is in the form $u_0(t)\phi_0(x)$, time and space components of the solution can be separated as follows:

$$\begin{aligned}&\mu\phi_0''''u_0 - \phi_0''u_0 + \phi_0\ddot{u}_0 = 0\\&\quad\Rightarrow \frac{1}{\mu}\frac{\ddot{u}_0}{u_0} = \frac{1}{\mu}\frac{\phi_0''}{\phi_0} - \frac{\phi_0''''}{\phi_0} = \lambda.\end{aligned} \tag{17}$$

This results in an eigenvalue problem where λ is the separation constant. The characteristic polynomial of the spatial problem is given by

$$r^4 - \frac{1}{\mu}r^2 + \lambda = 0. \tag{18}$$

The discriminant of this quartic polynomial is calculated as $\Delta = 16\lambda(4\lambda - \frac{1}{\mu^2})^2$. The function $\phi_0(x)$ is nontrivial only if $\Delta < 0$, which implies $\lambda < 0$. Consequently, the general form of the solution can be expressed as:

$$\begin{aligned}\phi_0(x) &= c_1 e^{-r_1 x} + c_2 e^{r_1 x} \\ &\quad + c_3 \sin(r_2 x) + c_4 \cos(r_2 x),\end{aligned} \tag{19}$$

where r_1 and r_2 are the roots of the characteristic polynomial (18), given by $r_1 = \sqrt{\frac{1+\sqrt{1-4\mu^2\lambda}}{2\mu}}$ and $r_2 = i\sqrt{\frac{-1+\sqrt{1-4\mu^2\lambda}}{2\mu}}$, with the remaining roots being $-r_1$ and $-r_2$. Applying the simply supported boundary conditions gives $c_1 = c_2 = c_4 = 0$. Furthermore, for nontrivial solutions of $\phi_0(x)$, r_2 must take the values $r_2 = n\pi$, for $n \in \mathbb{N}$. This condition implies that $\lambda = -(n^4\pi^4 + n^2\pi^2/\mu)$, which results in the corresponding eigenfunctions, up to an arbitrary multiplicative constant:

$$\phi_{0n}(x) = \sin(n\pi x). \tag{20}$$

Defining $\omega_n^2 := -\mu\lambda$, we obtain an expression for the natural frequency as

$$\omega_n = n\pi\sqrt{1 + \mu n^2\pi^2}. \tag{21}$$

Therefore, the temporal component of the solution is

$$u_{0n}(t) = \tilde{A}_n \sin(\omega_n t) + \tilde{B}_n \cos(\omega_n t), \tag{22}$$

where $\tilde{A}_n$ and $\tilde{B}_n$ are constants. Combining (20) and (22), the $\mathcal{O}(1)$ problem's solution can be obtained as:

$$v_s(x) + \sum_{n=1}^{\infty}[\tilde{A}_n \sin(\omega_n t) + \tilde{B}_n \cos(\omega_n t)]\sin(n\pi x). \tag{23}$$

Where a P-periodic function is defined as $f(x+P) = f(x)$ for a given period P, the eigenfunctions (20) are 2-periodic and odd in our spatial domain. However, (15) contains terms that are not odd (i.e. $\frac{\partial^2 v_0}{\partial x \partial t}$ and $\frac{\partial v_0}{\partial x}$). Multiplying these terms by the in x, 2-periodic function $\mathcal{H}(x)$ (see [32]), an equivalent expression that contains only odd terms can be obtained. The function $\mathcal{H}(x)$ is defined as:

$$\begin{aligned}\mathcal{H}(x) &= \sum_{j=0}^{\infty} \frac{4\sin((2j+1)\pi x)}{(2j+1)\pi} \\ &= \begin{cases} -1 \text{ for } -1 < x < 0, \\ \ \ 1 \text{ for } \ \ 0 < x < 1. \end{cases}\end{aligned} \tag{24}$$

Substituting (23) into (15) and using the orthogonality of the Fourier sine series in our spatial domain leads to secular terms in $v_1(x,t)$.

3.2 Multiple time scales method

For the proposed solution (12) to be qualified as an asymptotic approximation of the given problem, on a time-scale of order ε^{-1}, the secular terms in v_1 must be avoided. To achieve this, a two time-scales perturbation method will be applied. We introduce the time variables: $t_0 = t$ and $t_1 = \varepsilon t$ leading to:

$$\begin{aligned} &v_i(x,t) = v_i(x,t_0,t_1), \ \text{ for } i = \{0,1\} \\ &\frac{\partial}{\partial t} = \frac{\partial}{\partial t_0} + \varepsilon\frac{\partial}{\partial t_1}, \\ &\frac{\partial^2}{\partial t^2} = \frac{\partial^2}{\partial t_0^2} + 2\varepsilon\frac{\partial^2}{\partial t_0 \partial t_1} + \varepsilon^2\frac{\partial^2}{\partial t_1^2}. \end{aligned} \tag{25}$$

The function $v_0(x,t_0,t_1)$ is now given by

$$\begin{aligned} &v_0(x,t_0,t_1) \\ &\quad = \sum_{n=1}^{\infty}\left[A_n(t_1)\sin(\omega_n t_0) + B_n(t_1)\cos(\omega_n t_0)\right] \\ &\qquad \times \sin(n\pi x). \end{aligned} \tag{26}$$

Consequently, Eq. (15) becomes

$$\begin{aligned} &\mu\frac{\partial^4 v_1}{\partial x^4} - \frac{\partial^2 v_1}{\partial x^2} + \frac{\partial^2 v_1}{\partial t_0^2} \\ &\quad = -\alpha\frac{\partial^5 v_0}{\partial x^4 \partial t_0} - 2\frac{\partial^2 v_0}{\partial t_0 \partial t_1} \\ &\qquad - \sqrt{\beta}V_1\Omega\cos(\Omega t_0)\mathcal{H}(x)\frac{\partial v_0}{\partial x} \\ &\qquad - 2\sqrt{\beta}(V_0 + V_1\sin(\Omega t_0))\mathcal{H}(x)\frac{\partial^2 v_0}{\partial x \partial t_0}. \end{aligned} \tag{27}$$

We assume that $v_1(x,t_0,t_1) = \sum_{n=1}^{\infty} u_{1n}(t_0,t_1)\phi_{1n}(x)$ with $\phi_{1n}(x) = \sin(n\pi x)$. For visual simplicity, we will employ the notation $u_n(t_0,t_1)$ instead of

$u_{1n}(t_0, t_1)$. Substituting $v_0(x, t_0, t_1)$ into (27), and using the orthogonality of the Fourier sine series, the $\mathcal{O}(\varepsilon)$ equation can be derived as:

$$\begin{aligned}
&\frac{\partial^2 u_k}{\partial t_0^2} + \omega_k^2 u_k = \\
&\quad - \alpha\pi^4 k^4 \omega_k [A_k \cos(\omega_k t_0) - B_k \sin(\omega_k t_0)] \\
&\quad - 2\omega_k [\dot{A}_k \cos(\omega_k t_0) - \dot{B}_k \sin(\omega_k t_0)] \\
&\quad + \left(\sum_{2j+1+n=k} + \sum_{2j+1-n=k} - \sum_{2j+1-n=-k} \right) \frac{2\sqrt{\beta} V_1 k n}{n^2 - k^2} \\
&\quad \times \Big\{ (\Omega + 2\omega_n) \big[A_n \sin((\omega_n + \Omega) t_0) \\
&\qquad + B_n \cos((\omega_n + \Omega) t_0) \big] \\
&\qquad + (\Omega - 2\omega_n) \big[A_n \sin((\omega_n - \Omega) t_0) \\
&\qquad + B_n \cos((\omega_n - \Omega) t_0) \big] \Big\} \\
&\quad - \frac{8}{\pi} \sqrt{\beta} V_1 \Omega \cos(\Omega t_0) \\
&\quad \times \sum_{j=0}^{\infty} \frac{1}{2j+1} \int_0^1 v_s'(x) \sin((2j+1)\pi x) \sin(k\pi x) dx,
\end{aligned} \tag{28}$$

To provide a more compact notation, we define $\sum_n^* := \sum_{2j+1+n=k} + \sum_{2j+1-n=k} - \sum_{2j+1-n=-k}$ which indicates summation over indices satisfying $n \pm k$ is odd. For the same purpose, we also define the last term of Eq. (28)

$$\begin{aligned}
&C_k := \\
&\quad \sum_{j=0}^{\infty} \frac{1}{2j+1} \int_0^1 v_s'(x) \sin((2j+1)\pi x) \sin(k\pi x) dx,
\end{aligned} \tag{29}$$

where

$$\begin{aligned}
&\int_0^1 v_s'(x) \sin((2j+1)\pi x) \sin(k\pi x) dx \\
&= \begin{cases} \frac{4\gamma k (2j+1) \mu^2 \pi^2}{(1+(2j+1-k)^2 \mu\pi^2)(1+(2j+1+k)^2 \mu\pi^2)} \\ -\frac{4\gamma k (2j+1)}{\pi^2 (2j+1-k)^2 (2j+1+k)^2}, & k \text{ is even}, \\ 0, & k \text{ is odd}. \end{cases}
\end{aligned} \tag{30}$$

Notice that (30), and therefore C_k, depends linearly on $\gamma = \frac{m+M}{P} Lg$, the dimensionless gravitational constant. Thus, the presence of C_k results from accounting for the gravitational effect. Finding the exact values of C_k is not in the scope of this research, although, the proof of the convergence of the series C_k is presented in Appendix B. Thus, we refer to C_k as a nonzero constant for k is even and zero for k is odd. With this simplification, the $\mathcal{O}(\varepsilon)$ equation can be written as follows:

$$\begin{aligned}
&\frac{\partial^2 u_k}{\partial t_0^2} + \omega_k^2 u_k \\
&\quad = -\alpha\pi^4 k^4 \omega_k [A_k \cos(\omega_k t_0) - B_k \sin(\omega_k t_0)] \\
&\qquad - 2\omega_k [\dot{A}_k \cos(\omega_k t_0) - \dot{B}_k \sin(\omega_k t_0)] \\
&\qquad + \sum_{n=1}^{\infty}{}^* \sqrt{\beta} V_1 \frac{2kn}{n^2 - k^2} \\
&\qquad \times \Big\{ (\Omega + 2\omega_n) [A_n \sin((\omega_n + \Omega) t_0) \\
&\qquad + B_n \cos((\omega_n + \Omega) t_0)] \\
&\qquad + (\Omega - 2\omega_n) [A_n \sin((\omega_n - \Omega) t_0) \\
&\qquad + B_n \cos((\omega_n - \Omega) t_0)] \Big\} \\
&\qquad - \frac{8}{\pi} \sqrt{\beta} V_1 \Omega C_k \cos(\Omega t_0).
\end{aligned} \tag{31}$$

For $k = 1, 2, \ldots,$ Eq. (31) can be solved for each individual mode k. Depending on the value of Ω, the terms on the right-hand side (RHS) of Eq. (31) may align with the solutions of the homogeneous problem associated with Eq. (31), resulting in secular or unbounded solutions. These scenarios trivially occur for all k for first two terms on the RHS, and can also occur if $\omega_n \pm \Omega = \omega_K$ or if $\Omega = \omega_K$.

In Sect. 4, we investigate the individual occurrence of these secular terms. Moreover, in Sect. 6, we explore the more complex cases where multiple secular terms arise simultaneously, which can lead to complicated resonance behaviour.

4 Resonance frequencies

4.1 Determining resonance frequencies

In this section, we identify the fluid pulsation frequencies, Ω, that lead to secular terms in the solution. Since

$\sin(\omega_k t_0)$ and $\cos(\omega_k t_0)$ are in the kernel of Eq. (31), the occurrence of these terms in the RHS of (31) leads to secular terms in u_k. The excitation frequencies Ω that lead to secular terms in the solution are presented below:

- $\Omega = \omega_K$, where K is even and fixed. These frequencies correspond to primary resonances. This frequency follows from the last term in Eq. (31).
- $\Omega = \omega_L \pm \omega_M$, where $L \pm M$ is odd and L and M are fixed. These frequencies are referred to as combination resonances. This frequency follows from the indexing of $\sum^*$ in Eq. (31).

In this study, we also explore frequencies in the $\mathcal{O}(\varepsilon)$ neighbourhood of these resonances, which are usually referred to as the detuned frequencies.

Contrary to the studies in [31–33], we observe a resonant frequency $\Omega \simeq \omega_K$. Following from Eq. (31), the occurrence of this term is due to the inclusion of the potential energy contribution from gravity in our model.

Secondly, the eigenfunction choice made by [33] led to overlooking the orthogonality relations. This results in a failure to observe the rule that combination resonances must satisfy $K \pm N$ is odd. As a result, many nonexistent cases were reported (i.e. $K \pm N$ is even). Furthermore, in their study, the authors erroneously focused on so-called "principle parametric resonances $\Omega = 2\omega_K$", and "$\Omega = 0$ resonances" by considering $K = N$, which is shown in this paper and in [30,31,36,44] to be non-existent.

In the literature of pipes conveying pulsatile fluids, it is a common practice to consider only the first few modes, typically 2 or 4 (see the classical works in the field: [8–13,16–18], and more recent studies: [22–29]). After truncating the system to these lower modes, parametric and internal resonances are examined. However, as previously demonstrated in [31,32], and later in [33], higher-order modes that are neglected can be excited due to internal resonances for certain bending stiffness values μ. These cases are studied in detail in Sect. 6.

4.2 Non-resonant Ω

In situations where the fluid pulsation frequency Ω does not fall in the $\mathcal{O}(\varepsilon)$ neighbourhood of a resonance frequency, Eq. (31) becomes

$$\begin{aligned}\frac{\partial^2 u_k}{\partial t_0^2} + \omega_k^2 u_k &= -\alpha\pi^4 k^4 \omega_k [A_k \cos(\omega_k t_0) - B_k \sin(\omega_k t_0)] \\ &\quad - 2\omega_k [\dot{A}_k \cos(\omega_k t_0) - \dot{B}_k \sin(\omega_k t_0)] + \text{n.r.t.}\end{aligned} \tag{32}$$

Here "n.r.t." stands for the non-resonant terms. The secular terms in $u_k(t_0, t_1)$ can be avoided if $A_k(t_1)$ and $B_k(t_1)$ satisfies:

$$\dot{A}_k + \frac{\alpha\pi^4 k^4}{2} A_k = 0 \quad \text{and} \quad \dot{B}_k + \frac{\alpha\pi^4 k^4}{2} B_k = 0. \tag{33}$$

Therefore, the solutions for $A_k(t_1)$ and $B_k(t_1)$ are:

$$\begin{aligned} A_k(t_1) &= A_k(0) e^{-\frac{\alpha\pi^4 k^4}{2} t_1}, \\ B_k(t_1) &= B_k(0) e^{-\frac{\alpha\pi^4 k^4}{2} t_1}. \end{aligned} \tag{34}$$

These solutions exponentially converge to zero as $t \to \infty$ for all k, hence, v_0 converges to $v_s(x)$ as $t \to \infty$.

As it is introduced in this section 4, this section further explores the dynamics of the system under the resonant frequencies ω_K, $\omega_K \pm \omega_N$, and their ε neighborhoods.

4.3 Resonant Ω

4.3.1 The case $\Omega \simeq \omega_K$

We assume $\Omega \simeq \omega_K$ is an isolated resonance case, thus Ω is not $\mathcal{O}(\varepsilon)$ close to $\omega_K \pm \omega_N$ for any K, N.

Pure Resonance: $\Omega = \omega_K$

Initially, we investigate the scenario where the fluid pulsation frequency precisely matches a resonance frequency. Hence, substituting $\Omega = \omega_K$ for K is an even and fixed integer, and the equation with the terms that are leading to secular terms in $u_K(t_0, t_1)$ becomes:

$$\begin{aligned}&\frac{\partial^2 u_K}{\partial t_0^2}+\omega_K^2 u_K\\&\quad=-\alpha\pi^4K^4\omega_K[A_K\cos(\omega_K t_0)-B_K\sin(\omega_K t_0)]\\&\qquad-2\omega_K[\dot{A}_K\cos(\omega_K t_0)-\dot{B}_K\sin(\omega_K t_0)]\\&\qquad-\frac{8}{\pi}\sqrt{\beta}V_1\omega_K C_K\cos(\omega_K t_0)+\text{n.r.t.}\end{aligned}\tag{35}$$

Secular terms can be avoided in (35) if the following conditions are met:

$$\begin{aligned}&\dot{A}_K+\frac{\alpha\pi^4K^4}{2}A_K+\frac{4}{\pi}\sqrt{\beta}V_1C_K=0,\\&\dot{B}_K+\frac{\alpha\pi^4K^4}{2}B_K=0.\end{aligned}\tag{36}$$

Therefore, $A_K(t_1)$ and $B_K(t_1)$ must satisfy:

$$\begin{aligned}A_K(t_1)&=(A_K(0)+\frac{8\sqrt{\beta}V_1C_K}{\alpha\pi^5K^4})e^{-\frac{\alpha\pi^4K^4}{2}t_1}\\&\quad-\frac{8\sqrt{\beta}V_1C_K}{\alpha\pi^5K^4},\\B_K(t_1)&=B_K(0)e^{-\frac{\alpha\pi^4K^4}{2}t_1}.\end{aligned}\tag{37}$$

For all other $k\neq K$, $A_k(t_1)$ and $B_k(t_1)$ satisfy (34). As $t_0\to\infty$, $A_K\to-\frac{8\sqrt{\beta}V_1C_K}{\alpha\pi^5K^4}$ and $B_K\to 0$. Consequently, v_0 evolves towards a solution that exhibits oscillations around $v_s(x)$, with a fixed frequency ω_K.

Detuned Resonance: $\Omega=\omega_K+\varepsilon\varphi$

We now consider the excitation to be frequencies in the neighbourhood of the resonance frequency ω_K, defined as $\Omega=\omega_K+\varepsilon\varphi$, where φ is an $\mathcal{O}(1)$ detuning parameter and ε indicates that the detuning is $\mathcal{O}(\varepsilon)$. Then Eq. (31) can be obtained as

$$\begin{aligned}&\frac{\partial^2 u_K}{\partial t_0^2}+\omega_K^2 u_K\\&\quad=-\alpha\pi^4K^4\omega_K[A_K\cos(\omega_K t_0)-B_K\sin(\omega_K t_0)]\\&\qquad-2\omega_K[\dot{A}_K\cos(\omega_K t_0)-\dot{B}_K\sin(\omega_K t_0)]\\&\qquad-\frac{8}{\pi}\sqrt{\beta}V_1\omega_K C_K\cos(\omega_K t_0+\varphi t_1)+\text{n.r.t.}\end{aligned}\tag{38}$$

Using trigonometric identities, Eq. (38) can be rewritten as

$$\begin{aligned}&\frac{\partial^2 u_K}{\partial t_0^2}+\omega_K^2 u_K\\&\quad=\cos(\omega_K t_0)\big\{-\alpha\pi^4K^4\omega_K A_K-2\omega_K\dot{A}_K\\&\qquad-\frac{8}{\pi}\sqrt{\beta}V_1\omega C_K\cos(\varphi t_1)\big\}\\&\qquad+\sin(\omega_K t_0)\big\{\alpha\pi^4K^4\omega_K B_K+2\omega_K\dot{B}_K\\&\qquad+\frac{8}{\pi}\sqrt{\beta}V_1\omega C_K\sin(\varphi t_1)\big\}\\&\qquad+\text{n.r.t.}\end{aligned}\tag{39}$$

For the sake of simplicity, let us introduce the parameters:

$$a:=\frac{\alpha\pi^4K^4}{2},\quad c:=\frac{4}{\pi}\sqrt{\beta}V_1C_K.\tag{40}$$

Using this notation, we obtain

$$\begin{aligned}&\dot{A}_K=-aA_K-c\cos(\varphi t_1),\\&\dot{B}_K=-aB_K-c\sin(\varphi t_1).\end{aligned}\tag{41}$$

By using the method of integrating factors, one can solve the Eq. (41) as

$$\begin{aligned}A_K(t_1)&=-\frac{c}{a^2+\varphi^2}(a\cos(\varphi t_1)+\varphi\sin(\varphi t_1))\\&\quad+\left(A_K(0)+\frac{ac}{a^2+\varphi^2}\right)e^{-at_1},\\B_K(t_1)&=-\frac{c}{a^2+\varphi^2}(a\sin(\varphi t_1)-\varphi\cos(\varphi t_1))\\&\quad+\left(B_K(0)-\frac{\varphi c}{a^2+\varphi^2}\right)e^{-at_1}.\end{aligned}\tag{42}$$

The solution (42) indicates that the solution of (9)-(11) evolves into an oscillatory solution in the vicinity of the static solution $v_s(x)$.

4.3.2 The case $\Omega\simeq\omega_K-\omega_N$

We consider the combination resonance of difference type under the condition $K\pm N$ is odd. It is assumed in this section that $\Omega\simeq\omega_K-\omega_N$ represents an isolated resonance case. Therefore, all other possible resonance interactions are excluded.

Pure Resonance: $\Omega = \omega_K - \omega_N$

We first consider the pure resonance case. Substituting $\Omega = \omega_K - \omega_N$ into the Eq. (31), we obtain the system that A_K, B_K, A_N and B_N have to satisfy in order to avoid secular terms:

$$\begin{aligned}
\dot{A}_K &= -\frac{\alpha\pi^4K^4}{2}A_K + \sqrt{\beta}V_1\frac{KN(\omega_K+\omega_N)}{(N^2-K^2)\omega_K}B_N,\\
\dot{B}_K &= -\frac{\alpha\pi^4K^4}{2}B_K - \sqrt{\beta}V_1\frac{KN(\omega_K+\omega_N)}{(N^2-K^2)\omega_K}A_N,\\
\dot{A}_N &= -\frac{\alpha\pi^4N^4}{2}A_N + \sqrt{\beta}V_1\frac{KN(\omega_K+\omega_N)}{(N^2-K^2)\omega_N}B_K,\\
\dot{B}_N &= -\frac{\alpha\pi^4N^4}{2}B_N - \sqrt{\beta}V_1\frac{KN(\omega_K+\omega_N)}{(N^2-K^2)\omega_N}A_K.
\end{aligned} \tag{43}$$

Defining the following constants for simplicity:

$$\begin{aligned}
a &:= \frac{\alpha\pi^4K^4}{2}, \quad b := \frac{\alpha\pi^4N^4}{2},\\
p &:= \sqrt{\beta}V_1\frac{KN(\omega_K+\omega_N)}{(N^2-K^2)\omega_K},\\
q &:= \sqrt{\beta}V_1\frac{KN(\omega_K+\omega_N)}{(N^2-K^2)\omega_N}
\end{aligned} \tag{44}$$

we rewrite the Eq. (43) as:

$$\begin{pmatrix}\dot{A}_K\\ \dot{B}_K\\ \dot{A}_N\\ \dot{B}_N\end{pmatrix} = \begin{pmatrix}-a & 0 & 0 & p\\ 0 & -a & -p & 0\\ 0 & q & -b & 0\\ -q & 0 & 0 & -b\end{pmatrix}\begin{pmatrix}A_K\\ B_K\\ A_N\\ B_N\end{pmatrix}. \tag{45}$$

This system can be written as two, two-dimensional systems:

$$\begin{pmatrix}\dot{A}_K\\ \dot{B}_N\end{pmatrix} = \begin{pmatrix}-a & p\\ -q & -b\end{pmatrix}\begin{pmatrix}A_K\\ B_N\end{pmatrix}, \tag{46a}$$

$$\begin{pmatrix}\dot{B}_K\\ \dot{A}_N\end{pmatrix} = \begin{pmatrix}-a & -p\\ q & -b\end{pmatrix}\begin{pmatrix}B_K\\ A_N\end{pmatrix}. \tag{46b}$$

The given systems share the same characteristic polynomial, implying that the two systems have the same eigenvalues, and so, the same stability properties. The eigenvalues of the given system are given by

$$\lambda_{1,2} = -\frac{a+b}{2} \pm \frac{\sqrt{(a-b)^2-4pq}}{2}. \tag{47}$$

The exact solutions of (46) can be obtained by the given eigenvalues. Alternatively, since the systems are two dimensional, the stability condition can be given as

$$\begin{aligned}
\operatorname{tr}\begin{pmatrix}-a & p\\ -q & -b\end{pmatrix} &= -(a+b)\\
&= -\frac{\alpha\pi^4(K^4+N^4)}{2} < 0,
\end{aligned} \tag{48a}$$

$$\begin{aligned}
\det\begin{pmatrix}-a & p\\ -q & -b\end{pmatrix} &= ab + pq\\
&= \beta V_1^2\frac{K^2N^2}{(N^2-K^2)^2}\frac{(\omega_K+\omega_N)^2}{\omega_K\omega_N}\\
&\quad + \frac{\alpha^4\pi^8K^4N^4}{4} > 0.
\end{aligned} \tag{48b}$$

Since $\alpha, \beta > 0$, both inequalities are satisfied for all modes. Hence, the $\Omega = \omega_K - \omega_N$ scenario always leads to stable solutions. Therefore, the solution of (9)-(11) leads to the static solution for $t_0 \to \infty$ (where $\alpha > 0$).

Detuned Resonance: $\Omega = \omega_K - \omega_N + \varepsilon\varphi$

Introducing a small detuning parameter, $\varepsilon\varphi$, alters the dynamics of the system. Using the previously defined coefficients (see (44)), the system that has to be satisfied to prevent secular terms is given by:

$$\begin{aligned}
\dot{A}_K &= -aA_K + p\sin(\varphi t_1)A_N + p\cos(\varphi t_1)B_N,\\
\dot{B}_K &= -aB_K - p\cos(\varphi t_1)A_N + p\sin(\varphi t_1)B_N,\\
\dot{A}_N &= -bA_N - q\sin(\varphi t_1)A_K + q\cos(\varphi t_1)B_K,\\
\dot{B}_N &= -bB_N - q\cos(\varphi t_1)A_K - q\sin(\varphi t_1)B_K.
\end{aligned} \tag{49}$$

Notice that compared to system (47), system (52) is fully coupled. By differentiating the first two equations in (49), one obtains after applying some manipulations (see Appendix C), the following autonomous system:

$$\begin{aligned}
&\ddot{A}_K + (a+b)\dot{A}_K + (ab+pq)A_K\\
&\quad + \varphi(\dot{B}_K + aB_K) = 0,\\
&\ddot{B}_K + (a+b)\dot{B}_K + (ab+pq)B_K\\
&\quad - \varphi(\dot{A}_K + aA_K) = 0.
\end{aligned} \tag{50}$$

The characteristic polynomial of the given system is

$$\begin{aligned}&\lambda^4 + 2(a+b)\lambda^3 \\ &\quad + (\varphi^2 + (a+b)^2 + 2(ab+pq))\lambda^2 \\ &\quad + (2a\varphi^2 + 2(a+b)(ab+pq))\lambda \\ &\quad + (\varphi^2 a^2 + (ab+pq)^2) = 0.\end{aligned} \tag{51}$$

The roots of the quartic characteristic polynomial (51) are given by:

$$\begin{aligned}\lambda_1 &= -\frac{(a+b)}{2} + \frac{\varphi}{2}i \\ &\quad - \frac{1}{2}\sqrt{2\varphi(a-b)i + (a-b)^2 - 4pq - \varphi^2}, \\ \lambda_2 &= -\frac{(a+b)}{2} + \frac{\varphi}{2}i \\ &\quad + \frac{1}{2}\sqrt{2\varphi(a-b)i + (a-b)^2 - 4pq - \varphi^2}, \\ \lambda_3 &= -\frac{(a+b)}{2} - \frac{\varphi}{2}i \\ &\quad - \frac{1}{2}\sqrt{-2\varphi(a-b)i + (a-b)^2 - 4pq - \varphi^2}, \\ \lambda_4 &= -\frac{(a+b)}{2} - \frac{\varphi}{2}i \\ &\quad + \frac{1}{2}\sqrt{-2\varphi(a-b)i + (a-b)^2 - 4pq - \varphi^2}.\end{aligned} \tag{52}$$

For known parameter values, one can determine the roots (52) and the solutions of Eq. (50). Knowing A_K and B_K, one can obtain A_N and B_N from the expressions

$$\begin{aligned}A_N &= -\frac{1}{p}\Big[\sin(\varphi t_1)(\dot{A}_K + aA_K) \\ &\quad - \cos(\varphi t_1)(\dot{B}_K + aB_K)\Big], \\ B_N &= -\frac{1}{p}\Big[\cos(\varphi t_1)(\dot{A}_K + aA_K) \\ &\quad + \sin(\varphi t_1)(\dot{B}_K + aB_K)\Big].\end{aligned} \tag{53}$$

In order to define the stability of Eq. (50) and consequently of (49) for arbitrary parameter values, we study the real part of the eigenvalues obtained in (52), where the square root of a complex number is:

$$\begin{aligned}&\sqrt{A+Bi} = \\ &\pm\left(\sqrt{\frac{\sqrt{A^2+B^2}+A}{2}} + i\frac{B}{|B|}\sqrt{\frac{\sqrt{A^2+B^2}-A}{2}}\right),\end{aligned}$$

The eigenvalue with the largest real part has to satisfy the following condition in order to have stability:

$$\begin{aligned}&-\frac{(a+b)}{2} \\ &+\frac{1}{2\sqrt{2}}\Big(\sqrt{[(a-b)^2-\varphi^2-4pq]^2+4\varphi^2(a-b)^2} \\ &+(a-b)^2-4pq-\varphi^2\Big)^{\frac{1}{2}} < 0.\end{aligned} \tag{54}$$

This leads to the inequality

$$\varphi^2 > -(1+\frac{pq}{ab})(a+b)^2. \tag{55}$$

Where $a, b, (pq) > 0$, it is clear that the given inequality (55) holds for all parameter and detuning values. Therefore, we can conclude that the case $\Omega = \omega_K - \omega_N + \varepsilon\varphi$ is stable for all $\mathcal{O}(\varepsilon)$ detuned frequencies. This implies that the solution of (9)-(11) tends to the static solution for $t_0 \to \infty$.

4.3.3 The case $\Omega \simeq \omega_K + \omega_N$

Now we shall study the combination resonance of sum type under the condition $K \pm N$ is odd. We assume in this section that $\Omega \simeq \omega_K + \omega_N$ represents an isolated resonance case. Consequently, we exclude all other possible resonance interactions.

Pure Resonance: $\Omega = \omega_K + \omega_N$
Initially, we study the pure resonance case, where the excitation frequency is exactly equal to the sum of two natural frequencies. Substituting $\Omega = \omega_K + \omega_N$ into (31), we obtain a system of equations for $A_K(t_1)$, $B_K(t_1)$, $A_N(t_1)$ and $B_N(t_1)$ that has to be satisfied to avoid the occurrence of secular terms in $u_K(t_0, t_1)$ and $u_N(t_0, t_1)$:

$$
\begin{aligned}
\dot{A}_K &= -\frac{\alpha\pi^4K^4}{2}A_K + \sqrt{\beta}V_1\frac{KN(\omega_K-\omega_N)}{(N^2-K^2)\omega_K}B_N,\\
\dot{B}_K &= -\frac{\alpha\pi^4K^4}{2}B_K + \sqrt{\beta}V_1\frac{KN(\omega_K-\omega_N)}{(N^2-K^2)\omega_K}A_N,\\
\dot{A}_N &= -\frac{\alpha\pi^4N^4}{2}A_N + \sqrt{\beta}V_1\frac{KN(\omega_K-\omega_N)}{(N^2-K^2)\omega_N}B_K,\\
\dot{B}_N &= -\frac{\alpha\pi^4N^4}{2}B_N + \sqrt{\beta}V_1\frac{KN(\omega_K-\omega_N)}{(N^2-K^2)\omega_N}A_K.
\end{aligned}
\tag{56}
$$

For simplicity, we introduce the coefficients:

$$
\begin{aligned}
a &:= \frac{\alpha\pi^4K^4}{2}, \quad b := \frac{\alpha\pi^4N^4}{2},\\
p &:= \sqrt{\beta}V_1\frac{KN(\omega_K-\omega_N)}{(N^2-K^2)\omega_K},\\
q &:= \sqrt{\beta}V_1\frac{KN(\omega_K-\omega_N)}{(N^2-K^2)\omega_N}.
\end{aligned}
\tag{57}
$$

Using these coefficients, Eq. (56) can be written as:

$$
\begin{pmatrix}\dot{A}_K\\ \dot{B}_N\end{pmatrix} = \begin{pmatrix}-a & p\\ q & -b\end{pmatrix}\begin{pmatrix}A_K\\ B_N\end{pmatrix}, \tag{58a}
$$

$$
\begin{pmatrix}\dot{A}_N\\ \dot{B}_K\end{pmatrix} = \begin{pmatrix}-b & q\\ p & -a\end{pmatrix}\begin{pmatrix}A_N\\ B_K\end{pmatrix}. \tag{58b}
$$

The systems in Eq. (58) have the same characteristic polynomials, and so they have identical eigenvalues:

$$
\lambda_{1,2} = -\frac{a+b}{2} \pm \frac{\sqrt{(a-b)^2+4pq}}{2}. \tag{59}
$$

The stability of each system can be determined by the trace and the determinant of the matrices:

$$
\begin{aligned}
\operatorname{tr}\begin{pmatrix}-a & p\\ q & -b\end{pmatrix} &= -(a+b)\\
&= -\frac{\alpha\pi^4(K^4+N^4)}{2} < 0,
\end{aligned}
\tag{60a}
$$

$$
\begin{aligned}
\det\begin{pmatrix}-a & p\\ q & -b\end{pmatrix} &= ab-pq\\
&= -\beta V_1^2\frac{K^2N^2}{(N^2-K^2)^2}\frac{(\omega_K-\omega_N)^2}{\omega_K\omega_N}\\
&\quad + \frac{\alpha^2\pi^8K^4N^4}{4} > 0.
\end{aligned}
\tag{60b}
$$

Thus, the stability of the system for A_K, B_K, A_N and B_N is determined by

$$
\frac{\alpha^2\pi^8K^2N^2(N^2-K^2)^2\omega_K\omega_N}{4\beta V_1^2(\omega_K-\omega_N)^2} > 1. \tag{61}
$$

If the condition (61) is satisfied, then the $\mathcal{O}(1)$ solution of (9)-(11) converges to the static solution. However, for pipes with small viscoelastic damping α, (61) is not satisfied. As a result, the amplitude of the vibrations in (26) for modes K and N becomes unbounded.

Detuned Resonance: $\Omega = \omega_K + \omega_N + \varepsilon\varphi$

We now study the case where fluid velocity pulsation frequency is in the order ε neighbourhood of the sum of two natural frequencies. Substituting $\Omega = \omega_K + \omega_N + \varepsilon\varphi$ into Eq. (31), and using the notation introduced in (57), we obtain the fully coupled time-dependent system as

$$
\begin{aligned}
\dot{A}_K &= -aA_K - p\sin(\varphi t_1)A_N + p\cos(\varphi t_1)B_N,\\
\dot{B}_K &= -aB_K + p\cos(\varphi t_1)A_N + p\sin(\varphi t_1)B_N,\\
\dot{A}_N &= -bA_N - q\sin(\varphi t_1)A_K + q\cos(\varphi t_1)B_K,\\
\dot{B}_N &= -bB_N + q\cos(\varphi t_1)A_K + q\sin(\varphi t_1)B_K.
\end{aligned}
\tag{62}
$$

Following the same approach as in Appendix C, we obtain the following autonomous system of equations for A_K and B_K:

$$
\begin{aligned}
&\ddot{A}_K + (a+b)A_K + (ab-pq)A_K\\
&\quad + \varphi(\dot{B}_K + aB_K) = 0,\\
&\ddot{B}_K + (a+b)\dot{B}_K + (ab-pq)B_K\\
&\quad - \varphi(\dot{A}_K + aA_K) = 0.
\end{aligned}
\tag{63}
$$

The corresponding characteristic equation is:

$$
\begin{aligned}
&\lambda^4 + 2(a+b)\lambda^3\\
&\quad + (\varphi^2 + (a+b)^2 + 2(ab-pq))\lambda^2\\
&\quad + (2a\varphi^2 + 2(a+b)(ab-pq))\lambda\\
&\quad + (\varphi^2a^2 + (ab-pq)^2) = 0,
\end{aligned}
\tag{64}
$$

and the eigenvalues can be found as:

$$\begin{aligned}
\lambda_1 &= -\frac{(a+b)}{2} + \frac{\varphi}{2}i \\
&\quad - \frac{1}{2}\sqrt{2\varphi(a-b)i + (a-b)^2 + 4pq - \varphi^2}, \\
\lambda_2 &= -\frac{(a+b)}{2} + \frac{\varphi}{2}i \\
&\quad + \frac{1}{2}\sqrt{2\varphi(a-b)i + (a-b)^2 + 4pq - \varphi^2}, \\
\lambda_3 &= -\frac{(a+b)}{2} - \frac{\varphi}{2}i \\
&\quad - \frac{1}{2}\sqrt{-2\varphi(a-b)i + (a-b)^2 + 4pq - \varphi^2}, \\
\lambda_4 &= -\frac{(a+b)}{2} - \frac{\varphi}{2}i \\
&\quad + \frac{1}{2}\sqrt{-2\varphi(a-b)i + (a-b)^2 + 4pq - \varphi^2}.
\end{aligned} \tag{65}$$

Knowing A_K and B_K, one can also obtain A_N and B_N by substituting A_K and B_K into the expression

$$\begin{aligned}
A_N &= \frac{1}{p}\Big[\sin(\varphi t_1)\big(\dot{A}_K + aA_K\big) \\
&\quad - \cos(\varphi t_1)\big(\dot{B}_K + aB_K\big)\Big], \\
B_N &= -\frac{1}{p}\Big[\cos(\varphi t_1)\big(\dot{A}_K + aA_K\big) \\
&\quad + \sin(\varphi t_1)\big(\dot{B}_K + aB_K\big)\Big].
\end{aligned} \tag{66}$$

In order to define the stability of Eq. (60), we study the real part of the eigenvalues of (64) and we obtain the following condition for stability:

$$\varphi^2 > (a+b)^2\left(\frac{pq}{ab} - 1\right), \tag{67}$$

which can be written explicitly as

$$\begin{aligned}
\varphi^2 &> (K^4 + N^4)^2 \\
&\quad \times \left(\frac{\beta V_1^2(\omega_K - \omega_N)^2}{K^2N^2(N^2-K^2)^2\omega_K\omega_N} - \frac{\alpha^2\pi^8}{4}\right).
\end{aligned} \tag{68}$$

Solutions satisfying (68) converge to the static solution. However, if (68) is not satisfied, the amplitude of the vibrations of the modes K and N grows over time, implying that the system becomes unstable.

5 Transition across models

Following the examination of resonant frequencies, we investigate the influence of the bending stiffness $\mu = \frac{EI}{PL^2}$ on the characteristics of the solution of the governing partial differential equation. The order of the bending stiffness determines the transition between string, string-beam (or stretched beam) and beam models. In this section, we study the transition of models based on the natural frequency approximations, influenced by μ and the vibration mode number n. The concept of transition among bending stiffness and modes when studying parametric resonances relies on the studies of [42,43].

Large Bending Stiffness

For the case where the bending stiffness coefficient is large, $\mu \gg 1$, the expression for the natural frequency ω_n can be approximated by $\omega_n^{(\mathrm{b})}$ in the following way:

$$\begin{aligned}
\omega_n &= n\pi\sqrt{1 + \mu n^2\pi^2} \\
&= n^2\pi^2\sqrt{\mu} + \frac{1}{2\sqrt{\mu}} - \frac{1}{8\pi^2 n^2 \mu^{\frac{3}{2}}} + h.o.t., \\
\text{and } \omega_n^{(\mathrm{b})} &= n^2\pi^2\sqrt{\mu}.
\end{aligned} \tag{69}$$

Small Bending Stiffness

For a small bending stiffness coefficient, $\mu \ll 1$, the expression for the natural frequency ω_n can be approximated (for not too large n values) by $\omega_n^{(\mathrm{s})}$ in the following way:

$$\begin{aligned}
\omega_n &= n\pi + \frac{n^3\pi^3}{2}\mu - \frac{n^5\pi^5}{8}\mu^2 + h.o.t., \\
\omega_n^{(\mathrm{s})} &= n\pi.
\end{aligned} \tag{70}$$

In this study, we consider only a one-term approximation for the natural frequencies of the beam-like and string-like models. This choice is motivated by the fact that these single-term expansions correspond exactly to the natural frequency expressions of the pure beam or string models, making the physical interpretation of these frequencies straightforward. While including additional terms would extend the applicability of these models across a wider range of bending stiffness μ and

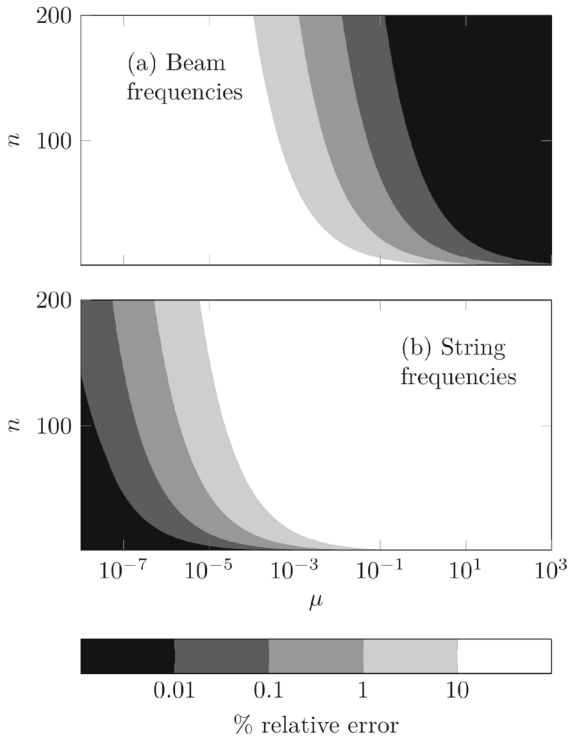

Fig. 2 The Figures **a** and **b** display the % relative error intervals for the natural frequency approximations for the beam like case and the string like case, respectively, for bending stiffness μ and mode number n

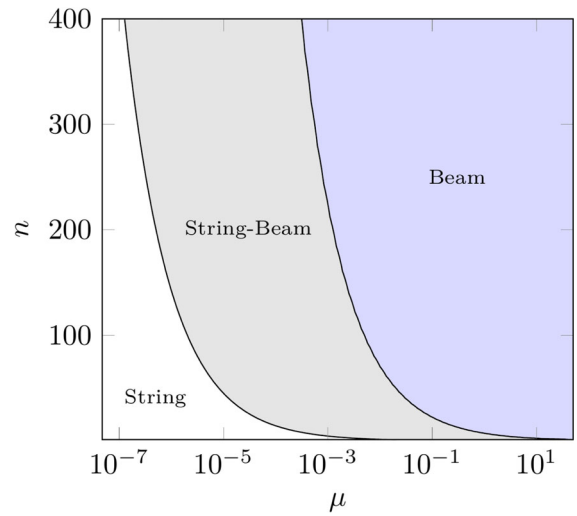

Fig. 3 1% relative error bounds in (μ, n) plane for string, string-beam and beam models

mode numbers n, it would also complicate the analytical expressions for special resonance conditions significantly.

In Fig. 2, the relative error intervals for the (69) and (70) choices for the exact natural frequencies are displayed.

At low μ values, the system behaves like a string for lower vibration modes. The accuracy of the string frequencies decreases as the mode number increases.

As μ or the mode number increases, a system transition from a string model to a stretch-beam model and a beam model occurs. For very large μ values, the beam model becomes valid for all vibration modes.

In Fig. 3, regions of string, stretch-beam and beam models are presented for 1% relative error bounds in the (μ, n) plane.

Note that the choice of 1% is arbitrary and serves as an illustrative example to demonstrate the transition among models. Different error bounds could be considered depending on specific application requirements, accuracy needs, or convenience.

It can be observed in Fig. 3 that for small μ values, up to a certain mode number, the system can be considered as a string-like problem. Upon this certain mode number, the string-like natural frequency approximations are no longer within the error bound concerning the exact natural frequency expression (21). Thus the stretched-beam modes are used. For even higher mode numbers, beam-like natural frequency approximations fall in the appropriate error bound. It can also be observed in Fig. 3 that, for $\mu > 0.0203$, the natural frequency of the system can no longer be approximated as string-like. Similarly, for $\mu > 49.8611$, the system can be approximated as beam-like for all mode numbers within the 1% relative error.

In the following section, we will analyze a simply supported pipe system using these three models. For small bending stiffness and up to a certain number of modes, the string model will be assumed valid. For large bending stiffness or higher mode numbers, the beam model will be assumed valid. For cases falling in between these limits, the stretched-beam model will be used.

6 Coinciding types of resonance frequencies

The resonant frequencies are found to be $\Omega = \omega_K, \omega_K - \omega_N, \omega_K + \omega_N$. However, for certain mode numbers and bending stiffness values, the fluid pulsation frequency Ω may align with multiple types of res-

Table 1 Special cases where different resonant frequencies coincide

Ω	ω_K	$\omega_K - \omega_N$	$\omega_K + \omega_N$
ω_L		Case-1	Case-2
$\omega_M - \omega_L$		Case-3	Case-5
$\omega_M + \omega_L$			Case-4

onance frequencies. In this section, these coincidences of resonance frequencies are investigated. Table 1 outlines possible coincidence scenarios.

The three models, namely the string, the string-beam and the beam models, exhibit distinct coincidence conditions. Therefore, in the following subsections, we investigate these coincidence cases for each pipe model.

6.1 The beam model ($\mu \gg 1$)

For the case where the bending stiffness coefficient $\mu \gg 1$, the expression for the natural frequency can be approximated by Eq. (69). It can be observed that the second term in the RHS of (69) is independent of the mode number. And so, very stiff pipes, the error compared to the exact natural frequency is $\mathcal{O}(1/\sqrt{\mu})$. In the case that $\omega_n = n^2\pi^2\sqrt{\mu}$, we shall study potential coincidences for different resonance frequencies described in table 1.

6.1.1 Coincidence case $\Omega \simeq \omega_K - \omega_N = \omega_L$

We assume that Ω does not lead to any other resonance interactions. The case $\Omega = \omega_K - \omega_N = \omega_L$ implies that

$$\begin{aligned} &\omega_K^{(\mathrm{b})} - \omega_N^{(\mathrm{b})} = \omega_L^{(\mathrm{b})} \\ &\quad \Leftrightarrow K^2\pi^2\sqrt{\mu} - N^2\pi^2\sqrt{\mu} = L^2\pi^2\sqrt{\mu} \\ &\quad \Leftrightarrow K^2 - N^2 = L^2 \end{aligned} \tag{71}$$

where L is even and $K \pm N$ is odd. Since $K \pm N$ is odd, $K^2 - N^2$ is odd. Conversely, since L is even, L^2 is even. The mismatch in parity leads to a contradiction. Thus, we conclude that the resonant case $\Omega = \omega_K - \omega_N = \omega_L$ cannot occur.

6.1.2 Coincidence case $\Omega \simeq \omega_K + \omega_N = \omega_L$

It is assumed that Ω is not $\mathcal{O}(\varepsilon)$-close to any other resonant frequencies, other than $\omega_K + \omega_N$ and ω_L. Similarly, the case $\Omega = \omega_K + \omega_N = \omega_L$ implies that

$$\omega_K^{(\mathrm{b})} + \omega_N^{(\mathrm{b})} = \omega_L^{(\mathrm{b})} \Leftrightarrow K^2 + N^2 = L^2. \tag{72}$$

Using the same approach, it is clear that the condition $K \pm N$ is odd implies that $K^2 + N^2$ is odd, which contradicts with the fact that L^2 is even. Therefore, the resonant case $\Omega = \omega_K + \omega_N = \omega_L$ cannot occur.

6.1.3 Coincidence case $\Omega \simeq \omega_K - \omega_N = \omega_M - \omega_L$

In this subsection, all other possible resonance interactions are excluded. This coincidence case can be generalized to the case of a coincidence of an arbitrary number of difference type combination resonances. Thus, consider

$$\Omega = \omega_{\xi_1}^{(\mathrm{b})} - \omega_{\eta_1}^{(\mathrm{b})} = \cdots = \omega_{\xi_n}^{(\mathrm{b})} - \omega_{\eta_n}^{(\mathrm{b})}, \tag{73}$$

$\xi_1, \ldots, \xi_n, \eta_1, \ldots, \eta_n \in \mathbb{N}$. Rewriting $\Omega = k\pi^2\sqrt{\mu}$ for $k \in \mathbb{N}$, implies

$$k = \xi_1^2 - \eta_1^2 = \cdots = \xi_n^2 - \eta_n^2. \tag{74}$$

Given that $\xi_i \pm \eta_i$ is odd, it follows that k must also be an odd integer. Writing the problem in the form

$$\begin{aligned} k &= (\xi_1 - \eta_1)(\xi_1 + \eta_1) \\ &\vdots \\ &= (\xi_n - \eta_n)(\xi_n + \eta_n) \end{aligned} \tag{75}$$

and defining the new variables $r_i, s_i \in \mathbb{N}$ as

$$\xi_i = \frac{r_i + s_i}{2}, \quad \eta_i = \frac{r_i - s_i}{2} \tag{76}$$

it follows that (74) can be rewritten as

$$k = r_1 s_1 = \cdots = r_n s_n. \tag{77}$$

Since $r_i = s_i$ yields to $\eta_i = 0$, it then follows that the number of modes excited corresponds to the number of non repeating divisors. Using the prime factorization $k = p_1^{\nu_1} p_2^{\nu_2} \ldots p_m^{\nu_m}$, the number of divisors of k is given

Table 2 Coincidences of the form $\omega_K^{(\mathrm{b})} - \omega_N^{(\mathrm{b})} = \omega_M^{(\mathrm{b})} - \omega_L^{(\mathrm{b})}$ for $\mu \gg 1$

k	$\Omega = k\pi^2\sqrt{\mu}$
15	$\omega_8 - \omega_7 = \omega_4 - \omega_1$
21	$\omega_{11} - \omega_{10} = \omega_5 - \omega_2$
27	$\omega_{14} - \omega_{13} = \omega_6 - \omega_3$
33	$\omega_{17} - \omega_{16} = \omega_7 - \omega_4$
35	$\omega_{18} - \omega_{17} = \omega_6 - \omega_1$
39	$\omega_{20} - \omega_{19} = \omega_8 - \omega_5$
45	$\omega_{23} - \omega_{22} = \omega_9 - \omega_6 = \omega_7 - \omega_2$
51	$\omega_{26} - \omega_{25} = \omega_{10} - \omega_7$
55	$\omega_{28} - \omega_{27} = \omega_8 - \omega_3$
57	$\omega_{29} - \omega_{28} = \omega_{11} - \omega_8$
63	$\omega_{32} - \omega_{31} = \omega_{12} - \omega_9 = \omega_8 - \omega_1$
65	$\omega_{33} - \omega_{32} = \omega_9 - \omega_4$
$\vdots$	$\vdots$

by $d_{\#}(k) = (\nu_1+1)(\nu_2+1)\ldots(\nu_m+1)$. Accordingly, the number of coincidence, n in (73), is:

$$n = \left\lfloor \frac{d_{\#}(k)}{2} \right\rfloor. \tag{78}$$

In table 2, some of the coincidence cases are given.

Additionally, from the asymptotic expression (69) for the natural frequency, it can be observed that assuming that $K^2 - N^2 = M^2 - L^2$, the given approximation for the resonance coincidence case $\Omega = \omega_K^{(\mathrm{b})} - \omega_N^{(\mathrm{b})} = \omega_M^{(\mathrm{b})} - \omega_L^{(\mathrm{b})}$ leads that

$$|(\omega_K - \omega_N) - (\omega_M - \omega_L)| = \mathcal{O}\left(\frac{1}{\mu^{\frac{3}{2}}}\right). \tag{79}$$

Notice that the coinciding frequencies have a higher order of accuracy, since

$$|\omega_n - \omega_n^{(\mathrm{b})}| = \mathcal{O}\left(\frac{1}{\sqrt{\mu}}\right).$$

Special Case $\Omega \simeq \omega_K - \omega_N = \omega_N - \omega_L$
We have shown that multiple differences in natural frequencies can coincide. We shall study whether two differences in natural frequencies can share a common frequency. It is clear that, for $\Omega = \omega_K^{(\mathrm{b})} - \omega_N^{(\mathrm{b})} = \omega_L^{(\mathrm{b})} - \omega_M^{(\mathrm{b})}$, $K = M \iff N = L$, which does not lead to any distinct combination resonance. Hence, the only possible coincidence case is when $M = N$, thus $\Omega = \omega_K^{(\mathrm{b})} - \omega_N^{(\mathrm{b})} = \omega_N^{(\mathrm{b})} - \omega_M^{(\mathrm{b})}$. This leads to the expression

$$K^2 + L^2 = 2N^2 \tag{80}$$

with the conditions; either K and L are odd and N is even, or K and L are even and N is odd.

- If K and L are odd, $K^2 + L^2$ becomes congruent to 2 modulo 4, while $2N^2$, with N even, is 0 modulo 4, which is a contradiction.
- If K and L are even, $K^2 + L^2$ becomes congruent to 0 modulo 4, while $2N^2$, with N odd, is 2 modulo 4, which is again a contradiction.

Hence, we conclude that coinciding differences in natural frequencies can not share a common mode.

The Dynamics for $\Omega \simeq \omega_K - \omega_N = \omega_M - \omega_L$
It has been shown that for this case the only possibility is that all the indices are distinct from each other. The dynamics for the given systems can be determined by using the solution approach given in section 4.3.2. Since, $\omega_K^{(\mathrm{b})} - \omega_N^{(\mathrm{b})}$ and $\omega_M^{(\mathrm{b})} - \omega_L^{(\mathrm{b})}$ do not share any common modes, the dynamics of the given system can be determined for the modes K, N, M, L by solving pairs of the modes K, N and M, L separately. Hence, we will not observe any distinct and unique dynamics of the system for the given internal resonances in this case.

6.1.4 The case $\Omega \simeq \omega_K + \omega_N = \omega_M + \omega_L$

Now we study the coincidence of combination resonances of sum type. This case includes only all other resonance interactions of same type. The binary quadratic form for as indefinite number of sum type combination resonances can be written as

$$\Omega = \omega_{\xi_1}^{(\mathrm{b})} + \omega_{\eta_1}^{(\mathrm{b})} = \cdots = \omega_{\xi_n}^{(\mathrm{b})} + \omega_{\eta_n}^{(\mathrm{b})}. \tag{81}$$

Considering $\Omega = k\pi^2\sqrt{\mu}$ with $k \in \mathbb{N}$ implies that

$$k = \xi_1^2 + \eta_1^2 = \cdots = \xi_n^2 + \eta_n^2. \tag{82}$$

Notice that $\xi \pm \eta$ being odd implies that k is odd. Defining $z_j := \xi_j + i\eta_j \in \mathbb{C}$, we can write the problem in

Table 3 Coincidences of the form $\omega_K^{(\mathrm{b})} + \omega_N^{(\mathrm{b})} = \omega_M^{(\mathrm{b})} + \omega_L^{(\mathrm{b})}$ for $\mu \gg 1$

k	$\Omega = k\pi^2\sqrt{\mu}$
65	$\omega_8 + \omega_1 = \omega_7 + \omega_4$
85	$\omega_9 + \omega_2 = \omega_7 + \omega_6$
125	$\omega_{11} + \omega_2 = \omega_{10} + \omega_5$
145	$\omega_{12} + \omega_1 = \omega_9 + \omega_8$
185	$\omega_{13} + \omega_4 = \omega_{11} + \omega_8$
205	$\omega_{14} + \omega_3 = \omega_{13} + \omega_6$
221	$\omega_{14} + \omega_5 = \omega_{11} + \omega_{10}$
265	$\omega_{16} + \omega_3 = \omega_{14} + \omega_8$
305	$\omega_{17} + \omega_4 = \omega_{16} + \omega_7$
325	$\omega_{18} + \omega_1 = \omega_{17} + \omega_6 = \omega_{15} + \omega_{10}$
⋮	⋮

Table 4 Coincidences of the form $\omega_K^{(\mathrm{b})} - \omega_N^{(\mathrm{b})} = \omega_M^{(\mathrm{b})} + \omega_L^{(\mathrm{b})}$ for $\mu \gg 1$

k	$\Omega = k\pi^2\sqrt{\mu}$
5	$\omega_3 - \omega_2 = \omega_2 + \omega_1$
13	$\omega_7 - \omega_6 = \omega_3 + \omega_2$
17	$\omega_9 - \omega_8 = \omega_4 + \omega_1$
25	$\omega_{13} - \omega_{12} = \omega_4 + \omega_3$
29	$\omega_{15} - \omega_{14} = \omega_5 + \omega_2$
37	$\omega_{19} - \omega_{18} = \omega_6 + \omega_1$
41	$\omega_{21} - \omega_{20} = \omega_5 + \omega_4$
45	$\omega_{23} - \omega_{22} = \omega_9 - \omega_6 = \omega_7 - \omega_2 = \omega_6 + \omega_3$
53	$\omega_{27} - \omega_{26} = \omega_7 + \omega_2$
61	$\omega_{31} - \omega_{30} = \omega_6 + \omega_5$
65	$\omega_{33} - \omega_{32} = \omega_9 - \omega_4 = \omega_8 + \omega_1 = \omega_7 + \omega_4$
73	$\omega_{37} - \omega_{36} = \omega_8 + \omega_3$
⋮	⋮

the form

$$k = z_1\bar{z}_1 = \cdots = z_n\bar{z}_n. \tag{83}$$

The pairs of z_i can be obtained by the Gaussian integer factorization of k, leading to the result that the integer k must be congruent 1 modulo 4. Thus, the number of distinct pairs is related to the number of prime divisors that are congruent to 1 modulo 4. A short list of indices giving rise to coincidences of sum type is presented in table 3 below:

Similarly to (79), for $K^2 + N^2 = M^2 + L^2$, we obtain the resonance coincidence approximation as

$$|(\omega_K + \omega_N) - (\omega_M + \omega_L)| = \mathcal{O}\left(\frac{1}{\mu^{\frac{3}{2}}}\right), \tag{84}$$

which represents a higher-order approximation for the coincidence compared to the order of accuracy for the beam frequency (69).

The Special Case $\Omega \simeq \omega_K + \omega_N = \omega_N + \omega_L$ We have demonstrated that multiple sums of natural frequencies can coincide. However, without loss of generality, the special case where $M = N$ is only possible if $K = L$ in $\Omega = \omega_K^{(\mathrm{b})} + \omega_N^{(\mathrm{b})} = \omega_M^{(\mathrm{b})} + \omega_L^{(\mathrm{b})}$. This equivalence implies that the condition does not correspond to a distinct pair of sums. Consequently, we can conclude that any two pairs of sums cannot share a common mode.

The Dynamics for $\Omega \simeq \omega_K + \omega_N = \omega_M + \omega_L$ Similar to 6.1.3, the dynamics for this case can be obtained individually for the pairs of modes K, N and M, L using the solutions and stability conditions presented in section 4.3.3.

6.1.5 The case $\Omega \simeq \omega_K - \omega_N = \omega_M + \omega_L$

In this subsection, we will study the case where the fluid pulsation frequency Ω is equal to the coincidence of a difference of two natural frequencies $\omega_K - \omega_N$ and a sum of two natural frequencies $\omega_M + \omega_L$. Let $\Omega = k\pi^2\sqrt{\mu}$, suppose k is an odd integer without any odd-powered prime factors congruent to 3 modulo 4. Consequently, k can be expressed as the sum of the squares of two integers. Since any odd number has at least one pair of factors (trivially, k has the divisors 1 and itself), following from Eq. (77) and (76), it can be written as the difference of two squares. This means that if the fluid pulsation frequency Ω is expressible as the sum of two natural frequencies, it can also be expressed as the difference of two natural frequencies. In table 4, some coincidence cases of sum and difference resonances are presented.

For the case $K^2 + N^2 = M^2 - L^2$ the resonance coincidence approximation is

$$|(\omega_K + \omega_N) - (\omega_M - \omega_L)| = \mathcal{O}\left(\frac{1}{\sqrt{\mu}}\right). \tag{85}$$

Special Case: $\Omega = \omega_K - \omega_N = \omega_N + \omega_L$
Note that in the given expression $\omega_K^{(\mathrm{b})} - \omega_N^{(\mathrm{b})} = \omega_M^{(\mathrm{b})} + \omega_L^{(\mathrm{b})}$, for positively defined ω_n, both sides of the equality can share a common mode only if $N = M$ or equivalently $N = L$. Without loss of generality, we assume $N = M$. This choice leads to the expression

$$K^2 = 2N^2 + L^2 \tag{86}$$

which is a well-known variation of the Pythagorean triples and can be solved using a modified version of Euclid's formula: $K = p^2 + 2m^2$, $N = 2mp$ and $L = |p^2 - 2m^2|$, where $p, m \in \mathbb{N}$. It can be seen that for odd integer values of p, the condition on the indices defined in $\sum^*$ is satisfied. Thus, we can conclude that this case leads to a special scenario, where the coinciding sum and difference combinations can share a common vibration mode.

It is straightforward to show that the coincidence of resonance frequencies cannot coincide with a third sum or difference type frequency with a common mode. Specifically, there are no P and Q such that $\omega_K - \omega_N = \omega_N + \omega_L = \omega_P \pm \omega_Q$, where P or Q are elements of $\{K, N, L\}$.

The Dynamics for $\Omega \simeq \omega_K - \omega_N = \omega_M + \omega_L$
The dynamics in the case for which all indices are distinct, follows from sections 4.3.3 and 4.3.2. However, when both systems share a common mode, we no longer can use these results. And so, a further analysis is required.

Pure Resonance: $\Omega = \omega_K - \omega_N = \omega_N + \omega_L$
First, the scenario where the fluid pulsation frequency Ω is exactly equal to $\omega_K^{(\mathrm{b})} - \omega_N^{(\mathrm{b})} = \omega_N^{(\mathrm{b})} + \omega_L^{(\mathrm{b})}$ is investigated. Substituting the excitation frequency into Eq. (31), we obtain that the following system of equations has to be satisfied in order to avoid the occurrence of secular terms in u_K, u_N and u_L:

$$\begin{aligned}
\dot{A}_K &= -\frac{\alpha\pi^4 K^4}{2} A_K + \sqrt{\beta} V_1 \frac{KN(\omega_K^{(\mathrm{b})} + \omega_N^{(\mathrm{b})})}{(N^2 - K^2)\omega_K^{(\mathrm{b})}} B_N, \\
\dot{B}_K &= -\frac{\alpha\pi^4 K^4}{2} B_K - \sqrt{\beta} V_1 \frac{KN(\omega_K^{(\mathrm{b})} + \omega_N^{(\mathrm{b})})}{(N^2 - K^2)\omega_K^{(\mathrm{b})}} A_N, \\
\dot{A}_N &= -\frac{\alpha\pi^4 N^4}{2} A_N + \sqrt{\beta} V_1 \frac{KN(\omega_K^{(\mathrm{b})} + \omega_N^{(\mathrm{b})})}{(N^2 - K^2)\omega_N^{(\mathrm{b})}} B_K \\
&\quad + \sqrt{\beta} V_1 \frac{NL(\omega_L^{(\mathrm{b})} - \omega_N^{(\mathrm{b})})}{(N^2 - L^2)\omega_N^{(\mathrm{b})}} B_L, \\
\dot{B}_N &= -\frac{\alpha\pi^4 N^4}{2} B_N - \sqrt{\beta} V_1 \frac{KN(\omega_K^{(\mathrm{b})} + \omega_N^{(\mathrm{b})})}{(N^2 - K^2)\omega_N^{(\mathrm{b})}} A_K \\
&\quad + \sqrt{\beta} V_1 \frac{NL(\omega_L^{(\mathrm{b})} - \omega_N^{(\mathrm{b})})}{(N^2 - L^2)\omega_N^{(\mathrm{b})}} A_L, \\
\dot{A}_L &= -\frac{\alpha\pi^4 L^4}{2} A_L + \sqrt{\beta} V_1 \frac{NL(\omega_L^{(\mathrm{b})} - \omega_N^{(\mathrm{b})})}{(N^2 - L^2)\omega_L^{(\mathrm{b})}} B_N, \\
\dot{B}_L &= -\frac{\alpha\pi^4 L^4}{2} B_L + \sqrt{\beta} V_1 \frac{NL(\omega_L^{(\mathrm{b})} - \omega_N^{(\mathrm{b})})}{(N^2 - L^2)\omega_L^{(\mathrm{b})}} A_N.
\end{aligned} \tag{87}$$

Introducing the coefficients,

$$\begin{aligned}
a &:= \frac{\alpha\pi^4 K^4}{2}, \quad b := \frac{\alpha\pi^4 N^4}{2}, \quad c := \frac{\alpha\pi^4 L^4}{2} \\
r &:= \sqrt{\beta} V_1 \frac{KN(\omega_K^{(\mathrm{b})} + \omega_N^{(\mathrm{b})})}{(N^2 - K^2)\omega_K^{(\mathrm{b})}}, \\
s &:= \sqrt{\beta} V_1 \frac{KN(\omega_K^{(\mathrm{b})} + \omega_N^{(\mathrm{b})})}{(N^2 - K^2)\omega_N^{(\mathrm{b})}}, \\
q &:= \sqrt{\beta} V_1 \frac{LN(\omega_L^{(\mathrm{b})} - \omega_N^{(\mathrm{b})})}{(N^2 - L^2)\omega_L^{(\mathrm{b})}}, \\
p &:= \sqrt{\beta} V_1 \frac{LN(\omega_L^{(\mathrm{b})} - \omega_N^{(\mathrm{b})})}{(N^2 - L^2)\omega_N^{(\mathrm{b})}},
\end{aligned} \tag{88}$$

Eq. (87) can be rewritten as two decoupled three dimensional systems

$$\begin{pmatrix} \dot{A}_K \\ \dot{B}_N \\ \dot{A}_L \end{pmatrix} = \begin{pmatrix} -a & r & 0 \\ -s & -b & p \\ 0 & q & -c \end{pmatrix} \begin{pmatrix} A_K \\ B_N \\ A_L \end{pmatrix}, \tag{89a}$$

$$\begin{pmatrix} \dot{B}_K \\ \dot{A}_N \\ \dot{B}_L \end{pmatrix} = \begin{pmatrix} -a & -r & 0 \\ s & -b & p \\ 0 & q & -c \end{pmatrix} \begin{pmatrix} B_K \\ A_N \\ B_L \end{pmatrix}. \tag{89b}$$

The two given systems lead to the same characteristic polynomial, which is

$$\begin{aligned}
&\lambda^3 + (a + b + c)\lambda^2 \\
&\quad + (ab + ac + bc - pq + rs)\lambda \\
&\quad + (abc - apq + crs) = 0.
\end{aligned} \tag{90}$$

In order to obtain an explicit expression for stability of system (87), we apply the Routh-Hurwitz criterion to the characteristic polynomial (90). For a general, cubic polynomial $d_3\lambda^3 + d_2\lambda^2 + d_1\lambda^1 + d_0 = 0$, the Routh-Hurwitz stability criterion is satisfied if $T_i > 0$, for $i = 0, 1, 2, 3$, where

$$T_0 = d_3, \quad T_1 = d_2,$$
$$T_2 = \det\begin{pmatrix} d_2 & d_3 \\ d_0 & d_1 \end{pmatrix}, T_3 = \det\begin{pmatrix} d_2 & d_3 & 0 \\ d_0 & d_1 & d_2 \\ 0 & 0 & d_0 \end{pmatrix}. \tag{91}$$

Using (91), we obtain for (90):

$$\begin{aligned} T_0 &= 1, \quad T_1 = a + b + c, \\ T_2 &= (a+b)(b+c)(a+c) \\ &\quad + (a+b)rs - (b+c)pq, \\ T_3 &= (abc - apq + crs) \\ &\quad \times [(a+b)(b+c)(a+c) \\ &\quad + (a+b)rs - (b+c)pq] \\ &= (abc - apq + crs)T_2. \end{aligned} \tag{92}$$

Assuming that the viscoelastic damping is not negligible, we have $a, b, c > 0$. Thus, we obtain as stability conditions $T_2 > 0$ and $(abc - apq + crs) > 0$.

Detuned Resonance: $\Omega = \omega_K - \omega_N + \varepsilon\varphi = \omega_N + \omega_L + \varepsilon\varphi$
Now we introduce an $\mathcal{O}(\varepsilon)$ deviation from the resonant frequency with the detuning $\varepsilon\varphi$. Substituting $\Omega = \omega_K - \omega_N + \varepsilon\varphi = \omega_N + \omega_L + \varepsilon\varphi$ into Eq. (31), we obtain the following system of equations that has to be satisfied:

$$\begin{aligned} \dot{A}_K &= -aA_K + r[\sin(\varphi t_1)A_N + \cos(\varphi t_1)B_N], \\ \dot{B}_K &= -aB_K - r[\cos(\varphi t_1)A_N - \sin(\varphi t_1)B_N], \\ \dot{A}_N &= -bA_N - s[\sin(\varphi t_1)A_K - \cos(\varphi t_1)B_K] \\ &\quad - p[\sin(\varphi t_1)A_L - \cos(\varphi t_1)B_L], \\ \dot{B}_N &= -bB_N - s[\cos(\varphi t_1)A_K + \sin(\varphi t_1)B_K] \\ &\quad + p[\cos(\varphi t_1)A_L + \sin(\varphi t_1)B_L], \\ \dot{A}_L &= -cA_L - q[\sin(\varphi t_1)A_K - \cos(\varphi t_1)B_K], \\ \dot{B}_L &= -cB_L + q[\cos(\varphi t_1)A_K + \sin(\varphi t_1)B_K], \end{aligned} \tag{93}$$

where the parameters, a, b, c, r, s, p, q are defined in (88). Observe that system (89) is obtained for $\varphi = 0$. After some manipulations (see Appendix D), we obtain an autonomous system of two third order equations:

$$\begin{aligned} \dddot{A}_N &= -(a+b+c)\ddot{A}_N \\ &\quad - (ab + ac + bc + rs - pq)\dot{A}_N \\ &\quad - (abc - apq + crs)A_N - \varphi^2(\dot{A}_N + BA_N) \\ &\quad - \varphi[(a-c)\dot{B}_N + (ab - bc + rs + pq)B_N], \\ \dddot{B}_N &= -(a+b+c)\ddot{B}_N \\ &\quad - (ab + ac + bc + rs - pq)\dot{B}_N \\ &\quad - (abc - apq + crs)B_N - \varphi^2(\dot{B}_N + bB_N) \\ &\quad + \varphi[(a-c)\dot{A}_N + (ab - bc + rs + pq)A_N]. \end{aligned} \tag{94}$$

Notice that the characteristic polynomial of Eq. (94) is of degree 6. Hence, for arbitrary parameter values, it is not feasible to determine the roots of the characteristic polynomial. Additionally, the Routh-Hurwitz stability conditions obtained for arbitrary parameters are too lengthy and complex for clear conclusions and comparisons. Therefore, the stability criterion will be studied through a specific example.

Example Case: $\Omega = \omega_3 - \omega_2 + \varepsilon\varphi = \omega_2 + \omega_1 + \varepsilon\varphi$
Considering the case where $\Omega = \omega_K - \omega_N + \varepsilon\varphi = \omega_N + \omega_M + \varepsilon\varphi$ where, $K = 3$, $N = 2$ and $M = 1$, we obtain the natural frequencies of these modes and coefficients defined in (88) as below:

$$\begin{aligned} &\omega_3 = 9\pi^2\sqrt{\mu}, \ \omega_2 = 4\pi^2\sqrt{\mu}, \ \omega_1 = \pi^2\sqrt{\mu}, \\ &a = \frac{81\pi^2\alpha}{2}, \ b = 8\pi^2\alpha, \ c = \frac{\pi^2\alpha}{2}, \\ &p = -\frac{\sqrt{\beta}V_1}{2}, \ q = -2\sqrt{\beta}V_1, \\ &r = -\frac{26\sqrt{\beta}V_1}{15}, \ s = -\frac{39\sqrt{\beta}V_1}{10}. \end{aligned} \tag{95}$$

If we substitute these into Eq. (94), we obtain the characteristic equation in the form

$$d_6\lambda^6 + d_5\lambda^5 + \cdots + d_1\lambda + d_0 = 0, \tag{96}$$

where the coefficients $d_i, i = 1, \ldots, 6$ are given in Appendix E. The region of stability for the given system in the parameters α and $\sqrt{\beta}V_1$ for various detuning values φ are presented in Fig. 4. The region below the curve —— indicates the stable region of the full system with $\Omega = \omega_3 - \omega_2 + \varepsilon\varphi = \omega_2 + \omega_1 + \varepsilon\varphi$ and the region

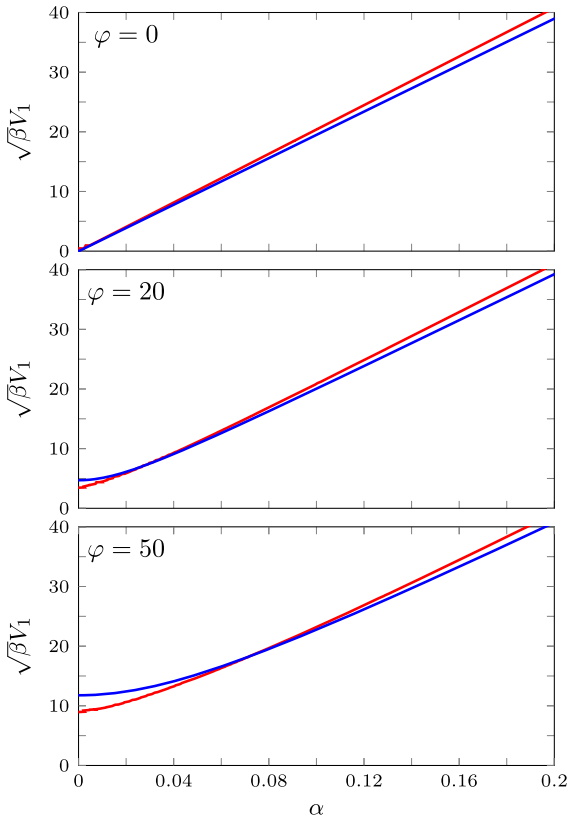

Fig. 4 Stability bounds for the system in modes $\{3, 2, 1\}$ —— and the truncated system in modes $\{2, 1\}$ ——. The stability region in the $(\alpha, \sqrt{\beta}V_1)$ plane is below each curve

below the curve —— indicates the stability region for the system truncated to the first two modes.

It can be observed from Fig. 4 that the truncation of the system influences the systems dynamics. In Sect. 6.2.5, a similar example for the same coincidence type of frequencies is presented, showing an even more clear influence on the stability regions (see Fig. 9).

6.2 The stretched-beam model ($\mu \sim 1$)

For the case where the amplitude of the bending stiffness coefficient μ is moderate, the natural frequency approximations used in Eq. (69) or Eq. (70) do not qualify to be asymptotic approximations. Hence, for this case, the natural frequency term is considered as the exact expression defined by (21). In the following subsections, resonant frequencies and the dynamics of the pipe structure under these resonance frequencies are investigated.

6.2.1 Coincidence case $\Omega \simeq \omega_K - \omega_N = \omega_L$

Any other potential resonance interactions, other than $\Omega \simeq \omega_K - \omega_N = \omega_L$, are disregarded.

We shall first examine, whether the coincidence under consideration is possible, or not. It is clear that the coincidence $\omega_K - \omega_N = \omega_L$, where $\omega_n = \pi n\sqrt{1 + \mu\pi^2 n^2}$, is possible only if $\omega_K > \omega_N$ and $\omega_K > \omega_L$ (or equivalently $K > N$ and $K > L$). In order to find cases satisfying this coincidence, we aim to get rid of the square root. Thus, we write

$$\begin{aligned}
&\omega_K - \omega_N = \omega_L \\
&\quad \Rightarrow \omega_K = \omega_N + \omega_L \\
&\quad \Rightarrow \omega_K^2 = \omega_N^2 + \omega_L^2 + 2\omega_N\omega_L \\
&\quad \Rightarrow (\omega_K^2 - \omega_N^2 - \omega_L^2)^2 = 4\omega_N^2\omega_L^2 \\
&\quad \Rightarrow \omega_K^4 + \omega_N^4 + \omega_L^4 \\
&\qquad - 2(\omega_K^2\omega_N^2 + \omega_K^2\omega_L^2 + \omega_N^2\omega_L^2) = 0,
\end{aligned} \tag{97}$$

which can be rewritten explicitly as

$$c_2\mu^2 + c_1\mu + c_0 = 0, \tag{98}$$

where $\mu = \frac{EI}{PL^2}$ is a real, positive, dimensionless constant, and

$$\begin{aligned}
c_0 &= \pi^4(K - N - L)(K - N + L) \\
&\quad \times (K + N - L)(K + N + L), \\
c_1 &= 2\pi^6\big(K^6 + N^6 + L^6 - K^4L^2 - K^4N^2 \\
&\quad - K^2L^4 - K^2N^4 - L^4N^2 - L^2N^4\big), \\
c_2 &= \pi^8(K^2 - N^2 - L^2)(K^2 - N^2 + L^2) \\
&\quad \times (K^2 + N^2 - L^2)(K^2 + N^2 + L^2).
\end{aligned} \tag{99}$$

Notice that this expression is equivalent to

$$\begin{aligned}
&(\omega_K - \omega_N - \omega_L)(\omega_K + \omega_N - \omega_L) \\
&\quad \times (\omega_K - \omega_N + \omega_L)(\omega_K + \omega_N + \omega_L) = 0.
\end{aligned} \tag{100}$$

This means that the expression (100) is also satisfied for other types of coincidences. However, the condition $\omega_K > \omega_N$ and $\omega_K > \omega_L$ implies that Eq. (97) is satisfied if and only if $\omega_K - \omega_N = \omega_L$. Hence, for each K, N, L, such that $K > N, L$, the μ value(s) that satisfy (98) can be calculated.

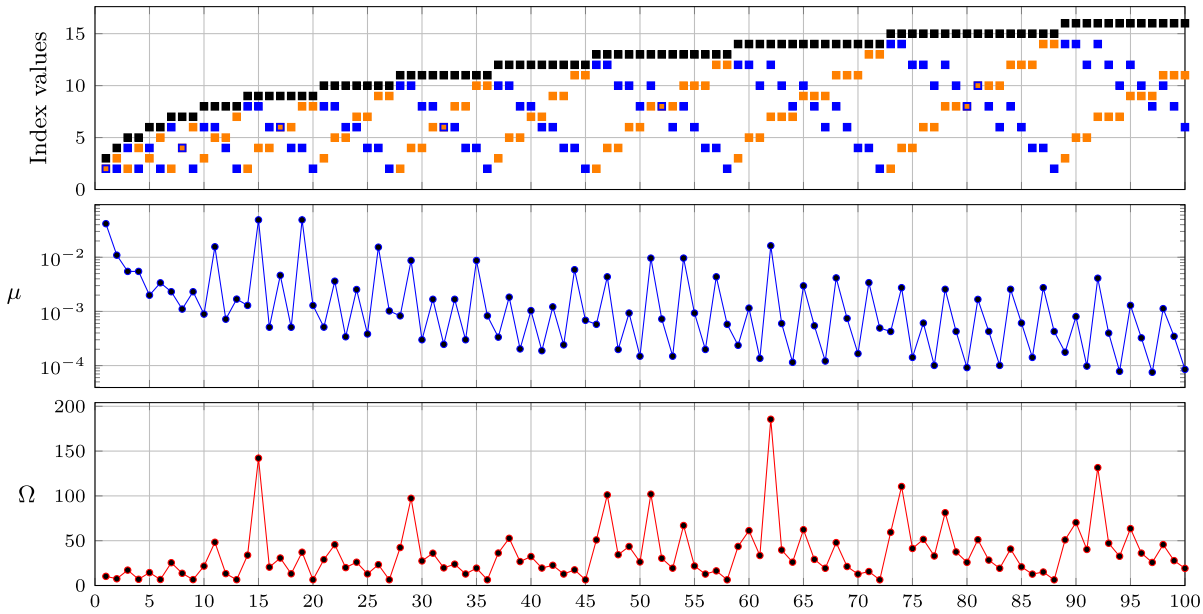

Fig. 5 Contributing modes of the first 100 coincidences: $\omega_{\blacksquare}$–$\omega_{\blacksquare}$=$\omega_{\blacksquare}$, with corresponding —●— μ and —●— Ω values

One observation is that a given resonance coincidence cannot contain the first mode. Since L is even, the only possibility is that $N = 1$ and K is even. If both K and L are even and $K > L$, it follows that $K \geq L + 2$. Using this relation, it is easy to see that $c_0 > 0$ and $c_2 > 0$. To prove that $c_1 > 0$, it is sufficient to write $K = L + 2 + m$ in (99), where $m \in \mathbb{N}$. Consequently, the roots of polynomial (98) are negative. This contradicts the fact that $\mu > 0$, and so the first mode cannot occur for the given resonance coincidence.

The Dynamics for $\Omega \simeq \omega_K - \omega_N = \omega_L$

As discussed earlier, when the index values K, N and L are all different, we obtain six ODEs. A system of four of these equations arises from $\Omega \simeq \omega_K - \omega_N$, while the remaining two form a two-dimensional system based on $\Omega \simeq \omega_L$. Consequently, the dynamics for each system can be solved using the corresponding individual equations, as explained earlier (see Sects. 4.3.1 and 4.3.2).

When $N = L$, it is clear that we no longer have a six-dimensional system that can be decoupled to a four-dimensional and to a two-dimensional system. Thus, when $N = L$ we cannot determine the dynamics of this system using the results from Sects. 4.3.1 and 4.3.2.

Special Case: $\Omega \simeq \omega_K - \omega_N = \omega_N$

Now we consider the special resonance case, where $N = L$, thus $\omega_K = 2\omega_N$. We can write

$$\begin{aligned} &\omega_K = 2\omega_N \\ &\quad \Rightarrow \pi K\sqrt{1+\mu\pi^2K^2} = 2\pi N\sqrt{1+\mu\pi^2N^2} \\ &\quad \Rightarrow K^2(1+\mu\pi^2K^2) = 4N^2(1+\mu\pi^2N^2), \end{aligned} \tag{101}$$

thus we obtain

$$\mu = \pi^2\frac{4N^2 - K^2}{K^4 - 4N^4}. \tag{102}$$

Eq. (102) leads to a physically meaningful solution only if $\mu > 0$. This condition is satisfied when $2N > K > \sqrt{2}N$.

The first 100 coincidence cases with indices K, N, L, and μ and Ω values for which the coincidence occurs are presented in Fig. 5. As an example, the 5th case occurs for indices $K = 6$, $N = 3$ and $L = 4$, and $\mu \simeq 1.9917$ and $\Omega \simeq 14.408$. Cases where $\omega_K - \omega_N = \omega_N$ are indicated by the nested markers $_{\blacksquare}$. For instance, the first coincidence case occurs for the indices $K = 3$, $N = L = 2$, $\mu \simeq 0.0417$ and $\Omega \simeq 10.223$. Similarly, for the indices $K = 15$, $N = L = 8$ (the 80th case) we see that $\mu \simeq 9.173 \cdot 10^{-5}$ and $\Omega \simeq 25.851$.

For the more interesting case, we now focus on the case $\omega_K - \omega_N = \omega_N$.

Pure Resonance: $\Omega = \omega_K - \omega_N = \omega_N$
Considering that $\Omega = \omega_K - \omega_N = \omega_N$, the coefficients $A_K(t_1)$, $B_K(t_1)$, $A_N(t_1)$ and $B_N(t_1)$ have to satisfy the following system of ODEs in order to avoid secular terms in $u_K(t_0, t_1)$ and $u_N(t_0, t_1)$:

$$\begin{aligned}
\dot{A}_K &= -\frac{\alpha\pi^4 K^4}{2} A_K + \sqrt{\beta} V_1 \frac{KN(\omega_K + \omega_N)}{(N^2 - K^2)\omega_K} B_N, \\
\dot{B}_K &= -\frac{\alpha\pi^4 K^4}{2} B_K - \sqrt{\beta} V_1 \frac{KN(\omega_K + \omega_N)}{(N^2 - K^2)\omega_K} A_N, \\
\dot{A}_N &= -\frac{\alpha\pi^4 N^4}{2} A_N + \sqrt{\beta} V_1 \frac{KN(\omega_K + \omega_N)}{(N^2 - K^2)\omega_N} B_K \\
&\quad - \frac{4}{\pi}\sqrt{\beta} V_1 C_N, \\
\dot{B}_N &= -\frac{\alpha\pi^4 N^4}{2} B_N - \sqrt{\beta} V_1 \frac{KN(\omega_K + \omega_N)}{(N^2 - K^2)\omega_N} A_K.
\end{aligned} \tag{103}$$

From the intermediate parameters defined in (40) and (44), we rewrite Eq. (103) as

$$\begin{aligned}
\begin{pmatrix} \dot{A}_K \\ \dot{B}_N \end{pmatrix} &= \begin{pmatrix} -a & p \\ -q & -b \end{pmatrix} \begin{pmatrix} A_K \\ B_N \end{pmatrix}, \\
\begin{pmatrix} \dot{B}_K \\ \dot{A}_N \end{pmatrix} &= \begin{pmatrix} -a & -p \\ q & -b \end{pmatrix} \begin{pmatrix} B_K \\ A_N \end{pmatrix} - \begin{pmatrix} 0 \\ c \end{pmatrix}.
\end{aligned} \tag{104}$$

The equilibrium of Eq. (104) is given by $A_K = B_N = 0$, $A_N = -\frac{ac}{ab+pq}$, $B_K = -\frac{pc}{ab+pq}$. The stability of this system is identical to that of the system described by Eq. (48b), indicating that it is stable.

Detuned Resonance: $\Omega \simeq \omega_K - \omega_N + \varepsilon\varphi = \omega_N + \varepsilon\varphi$
If the fluid velocity fluctuation frequency is detuned by $\Omega = \omega_K - \omega_N + \varepsilon\varphi = \omega_N + \varepsilon\varphi$ with $\varphi = \mathcal{O}(1)$, secular terms in $u_K(t_0, t_1)$ and $u_N(t_0, t_1)$ can be prevented if:

$$\begin{aligned}
\dot{A}_K &= -aA_K + p\sin(\varphi t_1)A_N + p\cos(\varphi t_1)B_N, \\
\dot{B}_K &= -aB_K - p\cos(\varphi t_1)A_N + p\sin(\varphi t_1)B_N, \\
\dot{A}_N &= -bA_N - q\sin(\varphi t_1)A_K + q\cos(\varphi t_1)B_K \\
&\quad - c\cos(\varphi t_1), \\
\dot{B}_N &= -bA_N - q\cos(\varphi t_1)A_K - q\sin(\varphi t_1)B_K \\
&\quad - c\sin(\varphi t_1).
\end{aligned} \tag{105}$$

Following the steps in Appendix C, the following system of two coupled second order ordinary differential equations for A_K and B_K can be obtained:

$$\begin{aligned}
&\ddot{A}_K + (a+b)\dot{A}_K + (ab+pq)A_K \\
&+ \varphi(\dot{B}_K + aB_K) = -cp\sin(2\varphi t_1), \\
&\ddot{B}_K + (a+b)\dot{B}_K + (ab+pq)B_K \\
&- \varphi(\dot{A}_K + aA_K) = cp\cos(2\varphi t_1),
\end{aligned} \tag{106}$$

Writing the above systems of ODEs in the form $L_1(A_K, B_K) = -cp\sin(2\varphi t_1)$ and $L_2(A_K, B_K) = cp\cos(2\varphi t_1)$, and differentiating each system once, we find:

$$L_1' = -2\varphi L_2 \text{ and } L_2' = 2\varphi L_1. \tag{107}$$

Note that the characteristic polynomial $P(\lambda)$ of the system $L_1 = 0$ and $L_2 = 0$ is equivalent to Eq. (51), with roots given by Eq. (52). And it has been proved in (55) that $\alpha > 0$ implies $\Re(\lambda) < 0$, where $\lambda \in \mathbb{C}$ such that $P(\lambda) = 0$. The characteristic polynomial $\widetilde{P}(\lambda)$ of (107) can be found to be:

$$\widetilde{P}(\lambda) = (\lambda^2 + 4\varphi^2)P(\lambda), \tag{108}$$

leading to the additional eigenvalues $\lambda_{5,6} = \pm 2\varphi i$. Since Eq. (107) is a linear system, the solution of the system has the same stability properties as system (49).

6.2.2 The case $\Omega \simeq \omega_K + \omega_N = \omega_L$

We exclude potential resonance interactions, other than $\Omega \simeq \omega_K + \omega_N = \omega_L$.

The resonance coincidence case, for which the sum of two natural frequencies is equal to a natural frequency is only possible if $\omega_L > \omega_K$ and $\omega_L > \omega_N$, thus for $L > K$ and $L > N$. And one observes that following the same steps, we obtain the expressions (97),(100) and (98). Hence, knowing K, N, L, one can obtain the μ value(s) that give rise to this type of resonance coincidence.

Similarly as in Sect. 6.2.1, the first mode cannot contribute to this given type of resonance coincidence. This statement can be proved by following the same approach as in Sect. 6.2.1.

Due to the conditions $\omega_L > \omega_K$ and $\omega_L > \omega_N$, thus $L > K$ and $L > N$, the given resonance coincidence can not lead to the special coincidence cases: $\omega_K + \omega_N = \omega_K$ or $\omega_K + \omega_N = \omega_N$.

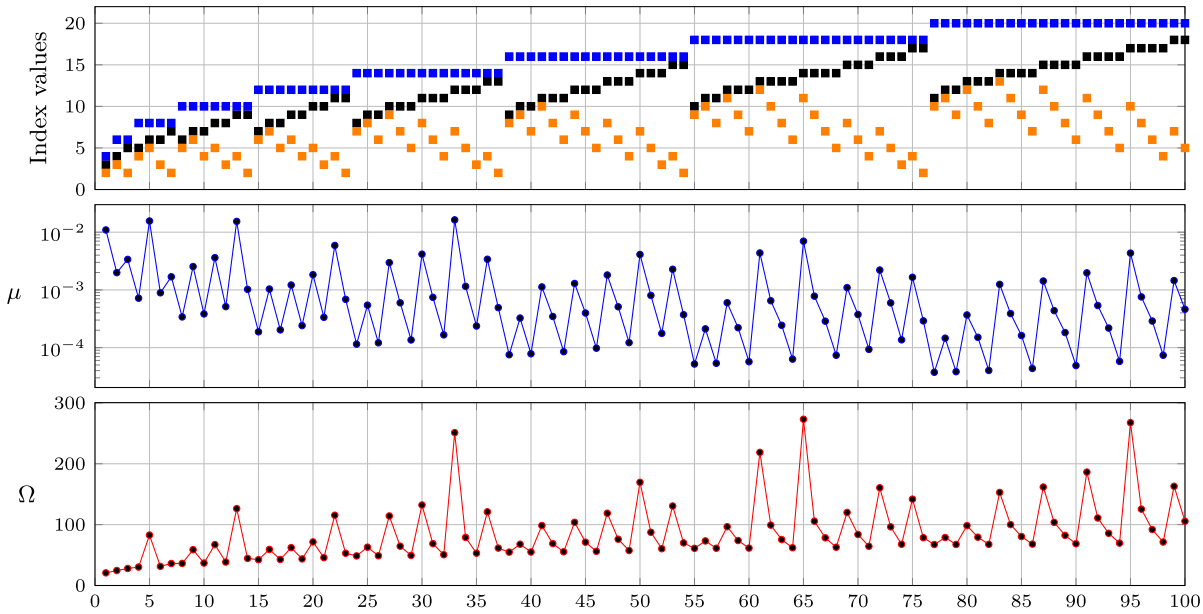

Fig. 6 Contributing modes to the first 100 coincidences: $\omega_{\blacksquare}+\omega_{\blacksquare}=\omega_{\blacksquare}$, with corresponding μ and Ω values

The first 100 coincidence cases with indices K, N, L, and μ and Ω values for which these coincidences occur, are presented in Fig. 6.

6.2.3 The case $\Omega \simeq \omega_K - \omega_N = \omega_M - \omega_L$

For this case, all other possible resonance interactions, other than $\Omega \simeq \omega_K - \omega_N = \omega_M - \omega_L$, are excluded.

Following a similar approach as in Sect. 6.2.1, the existence of a scenario where two differences of two natural frequencies are equal, requires solving a cubic polynomial in μ. Hence, in this section, the μ values giving rise to $\omega_K - \omega_N = \omega_M - \omega_L$, with K, N, M, L all different, are obtained numerically.

Given a resonance coincidence sharing a common mode is still to be figured out. As it has been shown in Sect. 6.1.3 that $K = M \iff N = L$, which does not provide a distinct system. Thus, the only scenario for which $\omega_K - \omega_N$ and $\omega_M - \omega_L$ share a common mode is that $N = M$. This choice leads to $\omega_K - \omega_N = \omega_N - \omega_L$, so $\omega_K + \omega_L = 2\omega_N$. The condition on the mode numbers is $\omega_K > \omega_N > \omega_L$ or equivalently $K > N > L$. Similarly as in Sect. 6.1.3, we obtain that the polynomial in μ is:

$$c_2\mu^2 + c_1\mu + c_0 = 0, \tag{109}$$

where

$$c_0 = \pi^4(K - 2N - L)(K - 2N + L) \times (K + 2N - L)(K + 2N + L), \tag{110a}$$

$$c_1 = 2\pi^6(K^2 + L^2 - 2N^2)\big(K^4 + L^4 - 8N^4 - 2K^2L^2 - 2K^2N^2 - 2L^2N^2\big), \tag{110b}$$

$$c_2 = \pi^8(K^2 - 2N^2 - L^2)(K^2 - 2N^2 + L^2) \times (K^2 + 2N^2 - L^2)(K^2 + 2N^2 + L^2). \tag{110c}$$

The given polynomial is equivalent to the expression

$$(\omega_K - 2\omega_N - \omega_L)(\omega_K + 2\omega_N - \omega_L) \times (\omega_K - 2\omega_N + \omega_L)(\omega_K + 2\omega_N + \omega_L) = 0. \tag{111}$$

Using the condition $\omega_K > \omega_N > \omega_L$, Eq. (111) indicates that Eq. (109) is satisfied either if $\omega_K + \omega_L - 2\omega_N = 0$ or if $\omega_K - \omega_L - 2\omega_N = 0$. Thus, for K, N, L and μ satisfying Eq. (109), one has to check what type of coincidence occurs. In Fig. 7, the first 100 coincidence cases with indices K, N, M, L, and μ and Ω values for which the coincidences occur, are presented. Cases where $N = M$ are indicated by the nested markers $\blacksquare$.

The Dynamics for $\Omega \simeq \omega_K - \omega_N = \omega_M - \omega_L$
In Sect. 4.3.2 it is observed that when the fluid pulsation

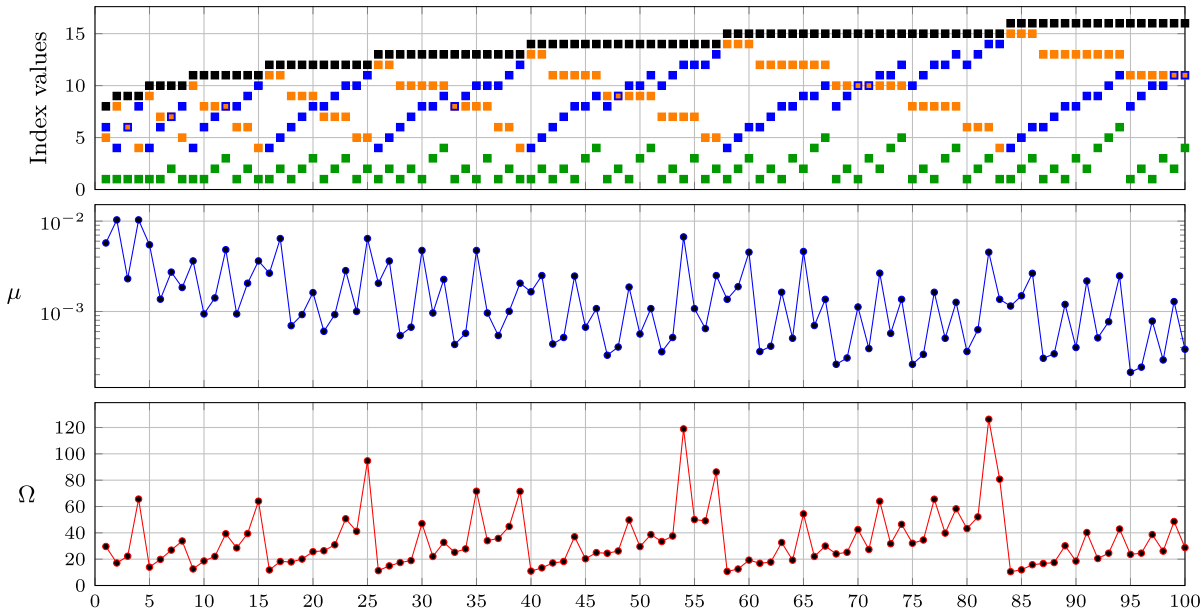

Fig. 7 Contributing modes to the first 100 coincidences: $\omega_{\blacksquare}$–$\omega_{\blacksquare}$ =$\omega_{\blacksquare}$–$_{\blacksquare}$, with corresponding —●— μ and —●— Ω values

frequency Ω is equal to the difference of two natural frequencies, the pipe system exhibits a stable behaviour for all parameter values. The dynamics for the cases where K, N, M, L are all different leads to two decoupled systems, studied in Sect. 4.3.2, and can be solved individually. Thus, we focus on the case where $N = M$, so $\Omega \simeq \omega_K - \omega_N = \omega_N - \omega_M$, which leads to a unique scenario.

Pure Resonance: $\Omega = \omega_K - \omega_N = \omega_N - \omega_L$
It is first assumed that the fluid pulsation frequency Ω is exactly equal to $\omega_K - \omega_N = \omega_N - \omega_L$. This assumption leads to the following system of ODEs that ensures that secular terms do not occur in $u_K(t_0, t_1)$,$u_N(t_0, t_1)$ and $u_L(t_0, t_1)$:

$$
\begin{aligned}
\dot{A}_K &= -\frac{\alpha\pi^4 K^4}{2} A_K + \sqrt{\beta} V_1 \frac{KN(\omega_K + \omega_N)}{(N^2 - K^2)\omega_K} B_N,\\
\dot{B}_K &= -\frac{\alpha\pi^4 K^4}{2} B_K - \sqrt{\beta} V_1 \frac{KN(\omega_K + \omega_N)}{(N^2 - K^2)\omega_K} A_N,\\
\dot{A}_N &= -\frac{\alpha\pi^4 N^4}{2} A_N + \sqrt{\beta} V_1 \frac{KN(\omega_K + \omega_N)}{(N^2 - K^2)\omega_N} B_K\\
&\quad - \sqrt{\beta} V_1 \frac{NL(\omega_N + \omega_L)}{(N^2 - L^2)\omega_N} B_L,\\
\dot{B}_N &= -\frac{\alpha\pi^4 N^4}{2} B_N - \sqrt{\beta} V_1 \frac{KN(\omega_K + \omega_N)}{(N^2 - K^2)\omega_N} A_K\\
&\quad + \sqrt{\beta} V_1 \frac{NL(\omega_N + \omega_L)}{(N^2 - L^2)\omega_N} A_L,\\
\dot{A}_L &= -\frac{\alpha\pi^4 L^4}{2} A_L + \sqrt{\beta} V_1 \frac{NL(\omega_N + \omega_L)}{(N^2 - L^2)\omega_L} B_N,\\
\dot{B}_L &= -\frac{\alpha\pi^4 L^4}{2} B_L - \sqrt{\beta} V_1 \frac{NL(\omega_N + \omega_L)}{(N^2 - L^2)\omega_L} A_N.
\end{aligned}
\tag{112}
$$

Introducing the parameters:

$$
\begin{aligned}
&a := \frac{\alpha\pi^4 K^4}{2}, \quad b := \frac{\alpha\pi^4 N^4}{2}, \quad c := \frac{\alpha\pi^4 L^4}{2},\\
&r := \sqrt{\beta} V_1 \frac{KN(\omega_K + \omega_N)}{(N^2 - K^2)\omega_K},\\
&s := \sqrt{\beta} V_1 \frac{KN(\omega_K + \omega_N)}{(N^2 - K^2)\omega_N},\\
&p := \sqrt{\beta} V_1 \frac{NL(\omega_N + \omega_L)}{(N^2 - L^2)\omega_N},\\
&q := \sqrt{\beta} V_1 \frac{NL(\omega_N + \omega_L)}{(N^2 - L^2)\omega_L}
\end{aligned}
\tag{113}
$$

System (112) becomes

$$\begin{pmatrix} \dot{A}_K \\ \dot{B}_K \\ \dot{A}_L \end{pmatrix} = \begin{pmatrix} -a & r & 0 \\ -s & -b & p \\ 0 & -q & -c \end{pmatrix} \begin{pmatrix} A_K \\ B_K \\ A_L \end{pmatrix}, \tag{114a}$$

$$\begin{pmatrix} \dot{B}_K \\ \dot{A}_K \\ \dot{B}_L \end{pmatrix} = \begin{pmatrix} -a & -r & 0 \\ s & -b & -p \\ 0 & q & -c \end{pmatrix} \begin{pmatrix} B_N \\ A_K \\ B_L \end{pmatrix}. \tag{114b}$$

The characteristic polynomial of both of these subsystems in (114) are identical, and are given by

$$\begin{aligned} &r^3 + (a+b+c)r^2 \\ &\quad + (ab+ac+bc+pq+rs)r \\ &\quad + (abc+apq+crs) = 0. \end{aligned} \tag{115}$$

One can define the roots of the characteristic polynomial by using Cardano's formula for the given parameter values. In order to obtain a manageable explicit expression for the stability of system (112), we apply the Routh-Hurwitz criterion to the characteristic polynomial (115). For a general, cubic polynomial $d_3 r^3 + d_2 r^2 + d_1 r^1 + d_0 = 0$, the Routh-Hurwitz stability criterion is satisfied if $T_i > 0$, for $i = 0, 1, 2, 3$, where T_i are defined in (91), and are given by:

$$\begin{aligned} T_0 &= 1, \quad T_1 = a+b+c, \\ T_2 &= (a+b)(b+c)(a+c) \\ &\quad + (b+c)pq + (a+b)rs, \\ T_3 &= (abc+apq+crs) \\ &\quad \times [(a+b)(b+c)(a+c) \\ &\quad + (b+c)pq + (a+b)rs]. \end{aligned} \tag{116}$$

Knowing that, $a, b, c, (pq), (rs)$ are all positive, real numbers, it follows that $T_i > 0$ for $i = 0, 1, 2, 3$, and so the system is stable.

Detuned Resonance: $\Omega = \omega_K - \omega_N + \varepsilon\varphi = \omega_N - \omega_L + \varepsilon\varphi$
Introducing a detuning of order ε, by $\varepsilon\varphi$, secular terms in $u_K(t_0, t_1)$,$u_N(t_0, t_1)$ and $u_L(t_0, t_1)$ are prevented if

$$\begin{aligned} \dot{A}_K &= -aA_K + r[\sin(\varphi t_1)A_N + \cos(\varphi t_1)B_N], \\ \dot{B}_K &= -aB_K - r[\cos(\varphi t_1)A_N - \sin(\varphi t_1)B_N], \\ \dot{A}_N &= -bA_N - s[\sin(\varphi t_1)A_K - \cos(\varphi t_1)B_K] \\ &\quad - p[\sin(\varphi t_1)A_L + \cos(\varphi t_1)B_L], \\ \dot{B}_N &= -bB_N - s[\cos(\varphi t_1)A_K + \sin(\varphi t_1)B_K] \\ &\quad + p[\cos(\varphi t_1)A_L - \sin(\varphi t_1)B_L], \\ \dot{A}_L &= -cA_L + q[\sin(\varphi t_1)A_N - \cos(\varphi t_1)B_N], \\ \dot{B}_L &= -cB_L + q[\cos(\varphi t_1)A_N + \sin(\varphi t_1)B_N], \end{aligned} \tag{117}$$

where the parameters a, b, c, r, s, p, q are given by (113). Following a similar approach as in Appendix D, we obtain the following autonomous system for A_N and B_N:

$$\begin{aligned} \dddot{A}_N &= -(a+b+c)\ddot{A}_N \\ &\quad - (ab+ac+bc+pq+rs)\dot{A}_N \\ &\quad - (abc+apq+crs)A_N - \varphi^2(\dot{A}_N + bA_N) \\ &\quad - \varphi[(a-c)\dot{B}_N + (ab-bc+rs-pq)B_N], \\ \dddot{B}_N &= -(a+b+c)\ddot{B}_N \\ &\quad - (ab+ac+bc+pq+rs)\dot{B}_N \\ &\quad - (abc+apq+crs)B_N - \varphi^2(\dot{B}_N + aB_N) \\ &\quad + \varphi[(a-c)\dot{A}_N + (ab-bc+rs-pq)A_N]. \end{aligned} \tag{118}$$

Similarly as for system (94), the characteristic polynomial obtained from system (118) is of degree 6. Therefore, an analytical study for arbitrary parameters is challenging. Hence, an example will be examined.

Example Case: $\Omega = \omega_9 - \omega_6 + \varepsilon\varphi = \omega_6 - \omega_1 + \varepsilon\varphi$
Taking $K = 9$, $N = 6$ and $L = 1$, the bending stiffness for which the coincidence occurs is:

$$\begin{aligned} \mu &= \frac{1}{44\pi^2} \simeq 0.002303, \\ \Omega &= \frac{21\pi\sqrt{55}}{22} = \simeq 22.2396, \\ \omega_9 &= \frac{45\pi\sqrt{55}}{22}, \quad \omega_6 = \frac{12\pi\sqrt{55}}{11}, \quad \omega_1 = \frac{3\pi\sqrt{55}}{22}, \\ a &= \frac{\alpha\pi^4 6561}{2}, \quad b = \alpha\pi^4 648, \quad c = \frac{\alpha\pi^4}{2}, \\ p &= \frac{27\sqrt{\beta}V_1}{140}, \quad q = \frac{54\sqrt{\beta}V_1}{35}, \\ r &= -\frac{46\sqrt{\beta}V_1}{25}, \quad s = -\frac{69\sqrt{\beta}V_1}{20}. \end{aligned} \tag{119}$$

And by applying the Routh-Hurwitz criterion, we obtain that the detuned system is stable for all α, $\sqrt{\beta}V_1$ and φ.

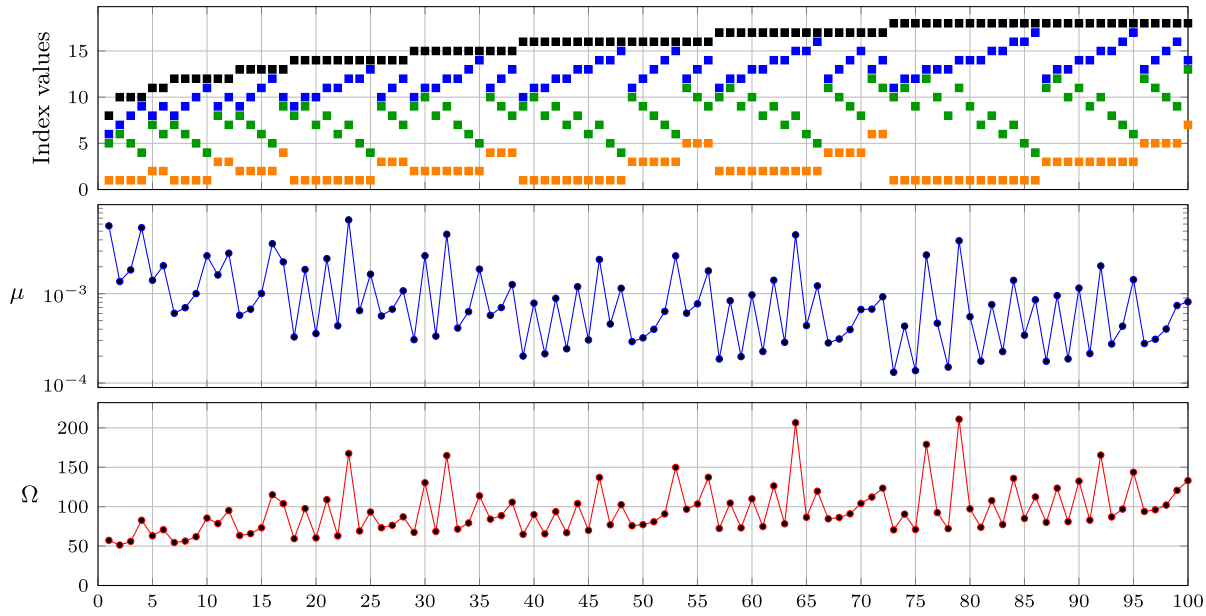

Fig. 8 Contributing modes of the first 100 coincidences: $\omega_{\blacksquare}+\omega_{\blacksquare}=\omega_{\blacksquare}+\omega_{\blacksquare}$, with corresponding μ and Ω values

6.2.4 The case $\Omega \simeq \omega_K + \omega_N = \omega_M + \omega_L$

In this subsection, the coincidences of two sums of two natural frequencies for moderate bending stiffness μ are investigated. We exclude the potential resonance interactions other than $\Omega \simeq \omega_K + \omega_N = \omega_M + \omega_L$. It is numerically obtained that (see Fig 8), the given coincidence type is possible. However, as it can be observed from section 6.1.4, for the given coincidence type, $N = M \iff K = L$. Therefore, the given frequency sums cannot share a common natural frequency.

Figure 8 displays the first 100 coincidence cases with indices K, N, M, L, and μ and Ω values for which the coincidences occur.

The Dynamics for $\Omega \simeq \omega_K + \omega_N = \omega_M + \omega_L$ Identical to Sect. 6.1.4, the dynamics for this case can be obtained individually for the pairs of modes K, N, and M, L using the solutions and stability conditions presented in section 4.3.3.

6.2.5 The case $\Omega \simeq \omega_K - \omega_N = \omega_M + \omega_L$

For a given resonance frequency, $\Omega \simeq \omega_K - \omega_N = \omega_M + \omega_L$, all other possible resonance interactions are disregarded. The coincidence for this type can be calculated numerically (see Fig. 10). The coincidence with a common mode, $N = M$, thus $\Omega \simeq \omega_K - \omega_N = \omega_N + \omega_L$ can be calculated analytically following Eq. (109), (110) and (111) from Sect. 6.2.3. In Fig. 10, the first 100 coincidence cases with indices K, N, M, L, and μ and Ω values for which the coincidences occur, are presented. Cases where $N = M$ and $N = L$ are indicated by the nested markers ■ and ■, respectively.

The Dynamics for $\Omega \simeq \omega_K - \omega_N = \omega_N + \omega_L$ The dynamics when $\Omega \simeq \omega_K - \omega_N = \omega_N + \omega_L$ and for $\mu \sim 1$ can be obtained similarly as for the case $\mu \gg 1$ in Sect. 6.1.5. Hence, no further analysis will be made. However, an example case will be given.

Example Case: $\Omega = \omega_5 - \omega_2 + \varepsilon\varphi = \omega_2 + \omega_3 + \varepsilon\varphi$ Following the same approach as in Sect. 6.1.5, it follows that the Routh-Hurwitz stability criterion (see appendix E) that the domain of stability can be computed, and is given in Fig. 9.

The stability region of the full system is indicated by the region below the curve ——, and the stability region of the truncated system is indicated by the region below the curve ——. For pure resonance ($\varphi = 0$), $\varphi = 20$ and $\varphi = 50$, the stability boundaries are illustrated. It can be observed that by truncating the system to a mode number, less than five, a different stability boundary is obtained for $\alpha > 0$.

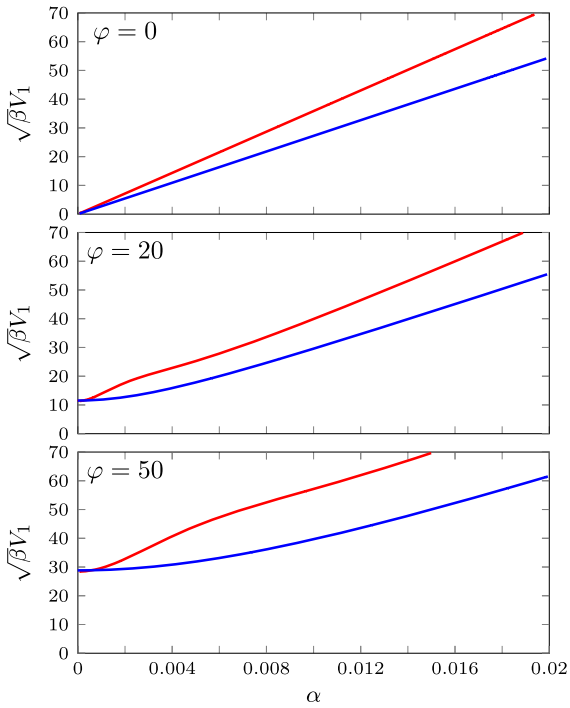

Fig. 9 Stability bounds for the full system of three modes {5, 3, 2} —— and the truncated system of two modes {3, 2} ——. Stability region in $(\alpha, \sqrt{\beta}V_1)$ plane is below each curve

6.3 The string model ($\mu \ll 1$)

When the bending stiffness coefficient $\mu \ll 1$, the natural frequency can be approximated by Eq. (70). From this approximation, $\omega_n^{(s)}$ is an $\mathcal{O}(n^3\mu)$ approximation of ω_n for small bending stiffness. This approximation is valid for all modes if $\mu = 0$, or for a limited number of modes if $\mu \neq 0$.

For $\omega_n \simeq \omega_n^{(s)} = n\pi$, we will examine potential resonances as shown in Table 1.

6.3.1 The case $\Omega \simeq \omega_K$

This scenario occurs only if K is even. It can be shown that there are no coinciding sum or difference-type combination resonances.

Given $\omega_a^{(s)} \pm \omega_b^{(s)} = \omega_{a\pm b}^{(s)}$ for all $a, b \in \mathbb{N}$, assume $\omega_K^{(s)} = \omega_N^{(s)} \pm \omega_L^{(s)}$ for K even and $N \pm L$ is odd. This implies:

$$\omega_K^{(s)} = \omega_N^{(s)} \pm \omega_L^{(s)} \Leftrightarrow K = N \pm L \tag{120}$$

which is a contradiction. Therefore, this resonance coincidence cannot occur.

Dynamics for $\Omega \simeq \omega_K$

The dynamics for this resonance frequency are identical to those in Sect. 4.3.1, and will not be further investigated here.

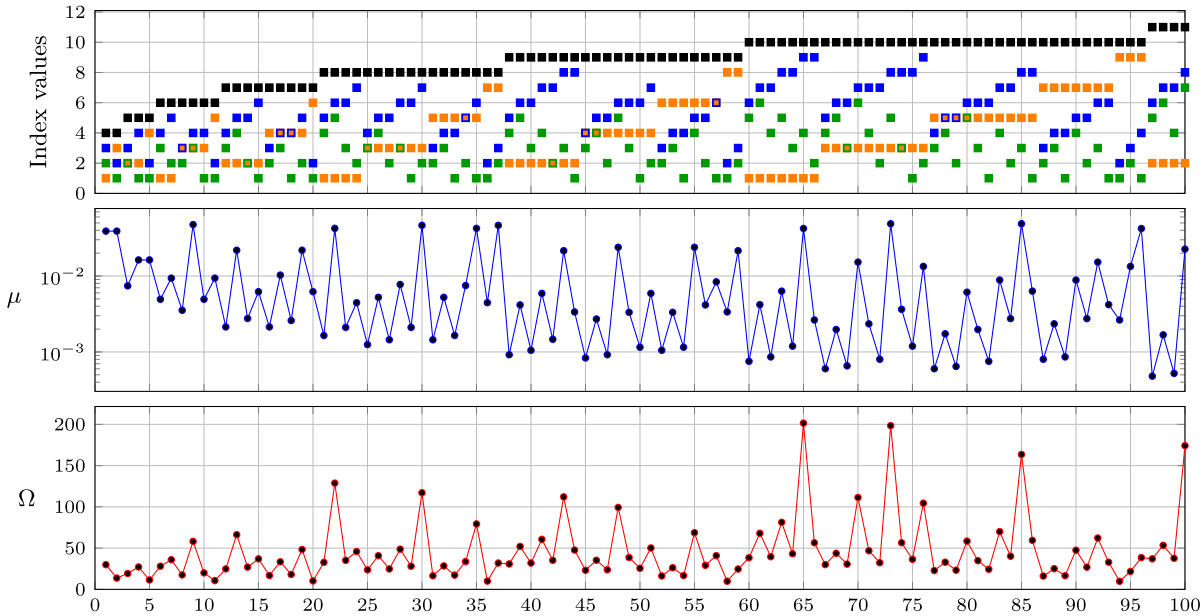

Fig. 10 Contributing modes of the first 100 coincidences:ω ■ -ω■=ω■ +■, with corresponding —●— μ and —●— Ω values

6.3.2 The case $\Omega \simeq \omega_K \pm \omega_N$

Assuming the fluid pulsation frequency equals a sum or difference type combination resonance, and since $\omega_K \pm \omega_N$ is only possible if $K \pm N$ is odd, we assume $\Omega \simeq m\pi$ for an odd integer m. Using $\omega_a^{(s)} \pm \omega_b^{(s)} = \omega_{a\pm b}^{(s)}$, we conclude that all pairs (K_i, N_i) such that $K_i \pm N_i = m$ lead to resonance. Therefore:

$$\begin{aligned}
\Omega = m\pi &= \omega_{m-1}^{(s)} + \omega_1^{(s)} \\
&= \omega_{m-2}^{(s)} + \omega_2^{(s)} \\
&\vdots \\
&= \omega_{\frac{m+1}{2}}^{(s)} + \omega_{\frac{m-1}{2}}^{(s)} \\
&= \omega_{m+1}^{(s)} - \omega_1^{(s)} \\
&= \omega_{m+2}^{(s)} - \omega_2^{(s)} \\
&\vdots
\end{aligned} \tag{121}$$

The first $\frac{m-1}{2}$ coincidences in (121) are of the sum type and the rest are difference-type combination resonances. This results in a fully coupled system of infinitely many ODEs. Two scenarios arise based on the bending stiffness: negligible ($\mu = 0$) and non-negligible ($\mu \neq 0$).

The Case $\mu = 0$
When $\mu = 0$, we have $\omega_n = \omega_n^{(s)} = n\pi$ for all $n \in \mathbb{N}$. This leads to an infinite-dimensional dynamical system. Suweken and van Horssen [30] studied a special case where viscoelastic damping is neglected ($\alpha = 0$) and $m = 1$ thus $\Omega = \pi$. They obtained the first integral of the infinite-dimensional system and found that truncated solutions fail to capture its dynamics accurately. While truncated systems exhibit bounded solutions regardless of the number of modes considered, the first integral of the complete system indicates that the energy of the system grows. Malookani and van Horssen later solved the infinite-dimensional problem employing the method of characteristic coordinates [40,41], verifying the results in [30]. The scenarios $\Omega = m\pi$ for $m > 1$ and $\alpha > 0$ remain as open problems.

The Case $\mu \neq 0$
Andrianov and van Horssen [42] and Ponomareva and van Horssen [43] observed that for $0 < \mu \ll 1$, the string-like natural frequency approximation is valid up to a certain mode number. Beyond this, modes follow a string-beam model, as discussed in Sect. 5. For small but nonzero bending stiffness, the coincidences in (121) hold only when $\omega_n^{(s)}$ is an adequate approximation of ω_n, resulting in a large but finite dynamical system for $A_k(t_1)$ and $B_k(t_1)$. Stability properties without viscoelastic damping have been investigated for various number of modes [43]. However, a comprehensive study on the stability of large systems considering viscoelastic damping remains open.

7 Numerical investigation

To support the analytical results, we performed numerical simulations using the Crank-Nicolson-like finite difference (FD) scheme. The scheme was selected for its stability and minimal dissipation characteristics. Alternative schemes, such as forward and backwards in time, were tested but discarded due to observed stability issues and excessive dissipation, making them unsuitable for the investigation. Further details on the numerical implementation are provided in Appendix F.

This section examines the resonance scenarios under various conditions and evaluates their stability properties. We first discuss the initial conditions and the steady-state solutions. Subsequently, the analysis focuses on the evolution of energy across different modes and their contributions to the system's overall stability.

7.1 Energy

The energy of each mode is assumed to be computed using the expressions in (2) and (3). Using the dimensionless coefficients, the total energy of the system at any time t is given by $E = T + V$ as:

$$\begin{aligned}
E(t) = \int_0^1 \Big(&\frac{\mu}{2} v_{xx}^2 + \frac{1+V^2}{2} v_x^2 + \frac{1}{2} v_t^2 \\
&+ \sqrt{\beta} V v_x v_t + \frac{V^2}{2} \Big) dx.
\end{aligned} \tag{122}$$

In this section, the primary focus is on modal interactions; therefore, the contribution of the potential energy due to gravity is omitted.

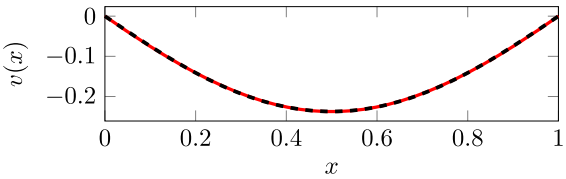

Fig. 11 Comparison of numerical - - - and analytical ——— static solutions

7.2 Initial conditions

The PDE under investigation (Eq. (9)) is non-homogeneous, leading to a non-zero stationary solution. The $\mathcal{O}(1)$ approximation of the static solution Eq.(16) can be replaced by the exact solution

$$\begin{aligned} v_s(x) = &-\frac{\gamma\mu}{1-\varepsilon^2 V_0^2}\operatorname{sech}\left(\frac{\sqrt{1-\varepsilon^2 V_0^2}}{2\sqrt{\mu}}\right) \\ &\times \cosh\left(\frac{(1-2x)\sqrt{1-\varepsilon^2 V_0^2}}{2\sqrt{\mu}}\right) \\ &+ \frac{\gamma}{2(1-\varepsilon^2 V_0^2)}(x^2 - x + 2\mu), \end{aligned} \tag{123}$$

due to the presence of $\mathcal{O}(\varepsilon^2)$ term as the coefficient of v_{xx} in Eq. (9). The consideration of the static solution is crucial for determining the initial conditions since it directly influences the initial energy of each vibration mode.

Figure 11 compares the analytically derived solution from Eq. (123) with the numerically calculated static solution. The two results match up to the fifth decimal place, demonstrating the accuracy of the numerical method.

To account for the energy contribution of the static solution, we define the initial conditions based on Eq. (11), as follows:

$$\begin{aligned} &v(x,0) = v_s(x) + v_0(x,t) + \varepsilon v_1(x,t) + \dots \\ &\quad \Rightarrow v_0(x,t) + \varepsilon v_1(x,t) + \dots = v(x,0) - v_s(x) \\ &\quad = \phi(x) - v_s(x), \\ &\quad v_t(x,0) = \psi(x), \end{aligned} \tag{124}$$

where $\phi(x)$ is the initial position of the pipe, and $\psi(x)$ is its initial velocity. Each mode contribution is then expressed as:

$$v(x,t) - v_s(x) = \sum_{j=1}^{N} A_j(t)\sin(j\pi x), \tag{125}$$

where $A_j(t)$ is the amplitude of mode j at time t and N is half the number of spatial grid points, based on the Nyquist criterion.

7.3 Numerical results

To support our analytical findings and validate the comments regarding [33] in Sect. 4, we numerically investigate the frequencies $\Omega = \omega_2$, $\Omega = \omega_2 + \omega_1$, $\Omega = 2\omega_1$, $\Omega = \omega_3 + \omega_1$ and a string-like resonance case $\Omega = \pi$. The first two cases demonstrate the results described in Sects. 4.3.1 and 4.3.3, respectively. The third and fourth cases are chosen to illustrate combination resonances of the form $\Omega = \omega_K \pm \omega_N$ where $K \pm N$ is even, aligning with the findings of [33]. The final case serves to confirm our conclusions for string-beam or stretched-beam systems.

The following parameters are used for the numerical simulations:

$$\begin{aligned} &\varepsilon = 0.01, \quad \gamma = 10, \quad \sqrt{\beta} = 0.5, \\ &V_0 = 20, \quad V_1 = 10 \end{aligned} \tag{126}$$

with numerical discretization parameters $\Delta x = 0.01$, $\Delta t = 0.001$. Given that the analytical studies are valid up to $\mathcal{O}(\frac{1}{\varepsilon})$, the temporal limit for the numerical integrations is set to $t = 100$.

The Case $\Omega = \omega_2 + \omega_1$

In this numerical example, we study the sum-type combination resonance of the first and second vibration modes. The bending stiffness is set large enough ($\mu = 1$) to ensure isolated resonance. Based on the analytical stability condition in Eq. (61), the required viscoelastic damping for stability is calculated to be $\alpha \simeq 0.0249$. Thus, we select two cases: $\alpha = 0.026$ and $\alpha = 0.023$, to demonstrate stable and unstable responses, respectively. In order to observe the modal interactions, the initial energy is allocated entirely to the first mode, with $E_1(0) = 1$.

The numerical results of cases $\alpha = 0.026$ and $\alpha = 0.023$ are presented in Fig. 12 and 13 respectively. For the stable case ($\alpha = 0.026$), the system's

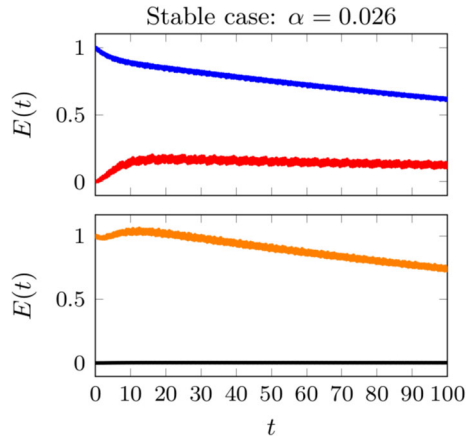

Fig. 12 Time evolution of $E_1(t)$ ▬, $E_2(t)$ ▬, total energy $E_{\text{total}}(t)$ ▬ and the energy of the remaining modes $E_{\text{total}}(t) - E_1(t) - E_2(t)$ ▬

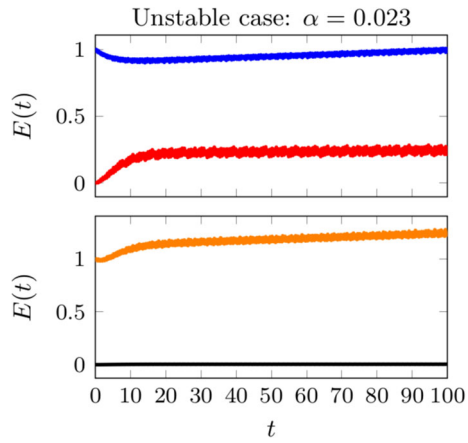

Fig. 13 Time evolution of $E_1(t)$ ▬, $E_2(t)$ ▬, total energy $E_{\text{total}}(t)$ ▬ and the energy of the remaining modes $E_{\text{total}}(t) - E_1(t) - E_2(t)$ ▬

total energy decays over time, as expected. In contrast, in an unstable case ($\alpha = 0.023$) the total energy grows. Furthermore, it is observed that energy is transferred from the first mode to the second mode, with these two modes accounting for most of the system's energy.

The Case $\Omega = \omega_2$

This resonance case tests the predictions in Sect. 4.3.1, namely $\Omega = \omega_K$ for K is even. According to the analysis, when the fluid pulsation frequency matches an even-numbered natural frequency, an oscillatory solution should occur near the static equilibrium. To test this, we assume zero initial energy ($E(0) = 0$), meaning that $v(x, 0) = v_s(x)$, and expect the solution to converge to the shifted equilibrium as described by Eq. (37).

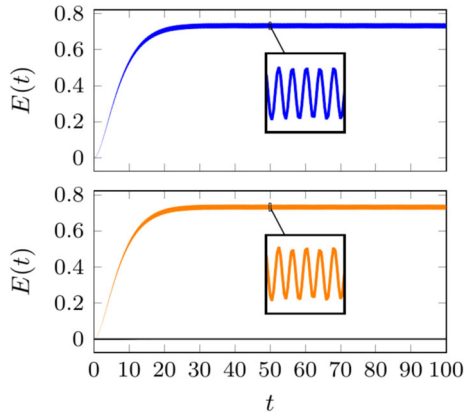

Fig. 14 Time evolution of $E_2(t)$ ▬, total energy $E_{\text{total}}(t)$ ▬, and the energy of the remaining modes $E_{\text{total}}(t) - E_2(t)$ ▬

The numerical results are shown in Fig. 14. Initially, all modes are set to zero. Over time, the energy of the second mode converges to a nonzero constant, while the energy of the remaining modes remains negligible. This confirms the predicted behaviour in Sect. 4.3.1.

The Case $\Omega = 2\omega_1$

In this example, we investigate the principal parametric resonance $\Omega = 2\omega_1$. Although this scenario is not observed in our analytical investigations, it was predicted by [33], which allows $K \pm N$ to be even for $\Omega = \omega_K \pm \omega_N$ (see Sect. 4.1 for details).

To observe the frequency response for the given pulsation frequency, we initiate the system with the energy of all modes set to zero ($E_i = 0$ for all i at $t = 0$), as previously done. A small damping coefficient is chosen, $\alpha = 10^{-4}$. It is expected that, if $\Omega = 2\omega_1$ is a resonant frequency, the energy of the first mode to turn up.

Figure 15 presents the results of the numerical integration. As shown, the first mode is not excited at the given fluid pulsation frequency. The energies across all modes remain below the order of 10^{-3}.

Figure 16 presents the results of the numerical integration with only the third mode excited to test whether the first mode could be excited due to other modes. It shows that while the energy of the third mode decays over time, the first mode remains unexcited.

Thus, Fig. 15 and 16 confirm that the given fluid pulsation frequency is not a resonant frequency, consistent with the analytical predictions from Sect. 4.1.

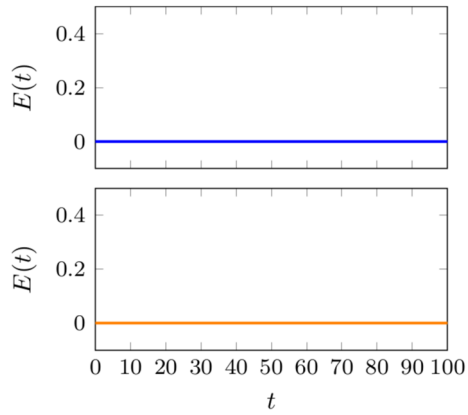

Fig. 15 Time evolution of $E_1(t)$ ▬, total energy $E_{\text{total}}(t)$ ▬, and the energy of the remaining modes $E_{\text{total}}(t) - E_1(t)$ ▬

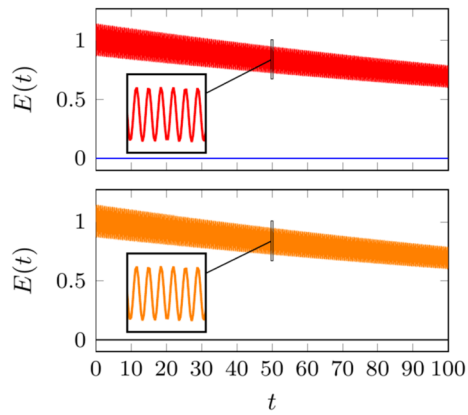

Fig. 16 Time evolution of $E_1(t)$ ▬, $E_3(t)$ ▬, total energy $E_{\text{total}}(t)$ ▬, and the energy of the remaining modes $E_{\text{total}}(t) - E_3(t)$ ▬

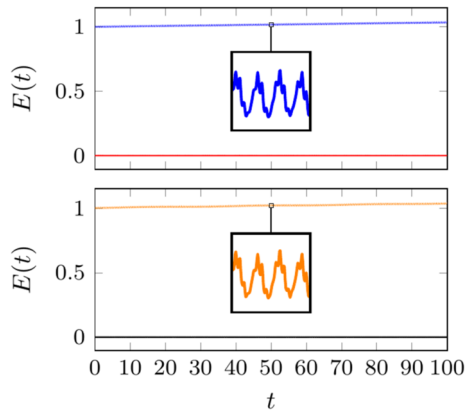

Fig. 17 Time evolution of $E_1(t)$ ▬, $E_3(t)$ ▬, total energy $E_{\text{total}}(t)$ ▬, and the energy of the remaining modes $E_{\text{total}}(t) - E_1(t)$ ▬

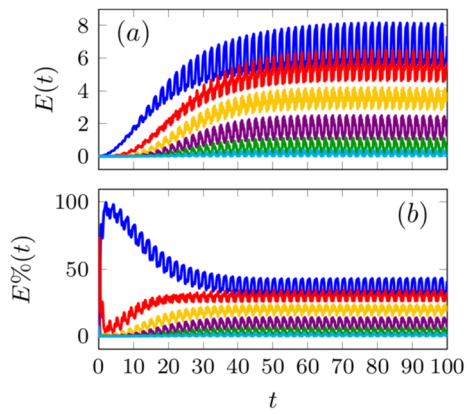

Fig. 18 **a** Time evolution of the energies of the first six modes: $E_1(t)$ ▬, $E_2(t)$ ▬, $E_3(t)$ ▬, $E_4(t)$ ▬, $E_5(t)$ ▬, $E_6(t)$ ▬. **b** Percentage contribution of each mode to the total energy over time

The Case $\Omega = \omega_3 + \omega_1$

In this example, we investigate another resonant frequency that is not observed in our analysis but was predicted by [33], for reasons similar to those discussed in the previous example and Sect. 4.1.

As in first numerical example ($\Omega = \omega_2 + \omega_1$), the initial energy is given only to the first mode, with $E_1(0) = 1$ and $E_i(0) = 0$ for $i > 1$. Again, a small damping coefficient, $\alpha = 10^{-4}$ is used.

The results of the numerical integration are shown in Fig. 17. The energy of the first mode, E_1, steadily increases over time. However, there is no significant increase in the energy of the third mode, E_3. As seen, E_1 contributes the most to the total energy of the system. This indicates that there is no interaction between modes 1 and 3, as predicted by our analysis in Sect. 4.1, and the energy remains concentrated primarily in the first mode.

The String-like Case $\Omega = \pi$

In this example, we conduct a numerical investigation for a system with small bending stiffness. As discussed in Sect. 6.3 and illustrated in Figs. 5, 7, and 10, it is analytically predicted that for small bending stiffness, multiple modes will be excited at specific fluid pulsation frequencies.

For this setup, we use the parameters $\alpha = 10^{-3}$, $\mu = 10^{-4}$ and $\Omega = \pi$ with the initial energy set to zero for all modes ($E_i(0) = 0$ for all i).

Figure 18 shows the numerical results, displaying the energy evolution of the first six modes. It is impor-

tant to note that while the remaining modes are also excited, their amplitudes are less than 1% of the total energy, and therefore are not shown here. As expected, all six modes are excited, confirming the analytical predictions in Sects. 6.2 and 6.3 for systems with small bending stiffness under this resonance condition.

8 Conclusions

In this paper, we investigated an initial-boundary value problem governing the dynamics of a simply supported pipe conveying fluid, modeled as an Euler-Bernoulli beam. The fluid flow velocity inside the pipe, $V(t)$, was assumed to be small and harmonically varying with frequency Ω: $V(t) = \varepsilon(V_0 + V_1 \sin(\Omega t))$, where $V_0 > |V_1|$ and $0 < \varepsilon \ll 1$. Although this study primarily focuses on the linear analysis of resonance conditions, the time-varying nature of the fluid velocity introduces parametric excitation into the system. This small harmonic variation introduces effects similar to nonlinear effects, such as complex resonance behaviour.

We examined potential resonance frequencies and studied modal interactions. When the fluid pulsation frequency Ω is not $\mathcal{O}(\varepsilon)$ close to any resonance frequency, the pipe system converges to its steady-state solution.

It was found that, with ω_K being the K-th natural frequency, the fluid pulsation frequencies $\Omega = \omega_K$ for K even, or $\Omega = \omega_K \pm \omega_N$ for $K \pm N$ odd, lead to resonances in the system. Excluding any additional resonance interactions, these three main resonances result in the following system dynamics:

- $\Omega = \omega_K$: A single mode is excited with no interaction between modes, resulting in an oscillatory state around a static solution.
- $\Omega = \omega_K - \omega_N$: Two modes are excited, with interaction between modes K and N. The system remains stable for all parameter values.
- $\Omega = \omega_K + \omega_N$: Two modes are excited, with interaction between modes K and N. The system is conditionally stable depending on parameter values.

Depending on the order of bending stiffness μ, special resonance coincidence cases were investigated for beam ($\mu \gg 1$), string-beam ($\mu \sim 1$), and string ($\mu \ll 1$) models, each displaying unique resonance behaviour. The transitions between these models were discussed: for lower μ values and mode numbers, the system behaves like a string; if the mode number increases or higher bending stiffness values are considered, then the vibration modes change into string-beam and beam-like behaviour.

- $\boldsymbol{\mu \gg 1}$ **:** The beam model can excite up to three coupled modes and an indefinite number of decoupled modes by interactions among combination resonances.
- $\boldsymbol{\mu \sim 1}$ **:** The stretched-beam model exhibits a richer spectrum of resonance coincidences, occurring from all possible pairwise combinations of resonance frequencies, with up to three coupled modes or four modes in a 2-2 coupled form.
- $\boldsymbol{\mu \ll 1}$ **:** The string model can lead to various resonance scenarios, exciting a single mode via $\Omega = \omega_K$ or through any combination resonance. The latter type can involve infinitely many ($\mu = 0$) or a large number of interactions ($\mu \neq 0$).

For beam and stretched-beam models, all resonance scenarios, inducing detuned resonances are investigated. Example cases of three-mode interactions were provided with truncated solutions for comparison. For the string model, potential resonance scenarios were presented, and existing solutions in the literature were discussed. It was observed in this study that early truncation can result in neglecting higher-order modal interactions, leading to incorrect solutions or stability results. These findings highlight the limitations of the Galerkin truncation method in parametric resonance studies, as it fails to capture higher-order mode interactions that are critical for the system's dynamics.

Future studies could extend this approach to the string model for pipes, which presents more challenges. The approach could be extended for the fluid flow velocity with a moderate amplitude, for instance, $V(t) = V_0 + \varepsilon V_1 \sin(\Omega t)$. Additionally, different boundary conditions and nonlinear equations of motion could be explored. Finally, coincidence scenarios where resonance frequencies are not exactly equal but within each other's $\mathcal{O}(\varepsilon)$ neighbourhoods, such that $\Omega = \omega_{K_1} \pm \omega_{N_1} = \omega_{K_2} \pm \omega_{N_2} + \varepsilon\varphi_1 = \cdots = \omega_{K_{n+1}} \pm \omega_{N_{n+1}} + \varepsilon\varphi_n$, can be studied.

Author contributions Both authors contributed equally to all aspects of the paper.

Funding This research received no specific grant from any funding agency.

Data Availability Statement No datasets were generated or analysed during the current study.

Declarations

Conflict of interest The authors declare no competing interests.

Appendix A

In this appendix, the intermediate steps between Eq. (13) and Eq. (16) are presented. (13) being $\mu v_s''''(x) - v_s''(x) + \gamma = 0$, defining a new function as $\xi(x) := v_s''(x) - \gamma$, we obtain a second order homogeneous ode for $\xi(x)$ as

$$\mu\xi''(x) - \xi(x) = 0. \tag{A1}$$

Eq. (A1) can be solved as

$$\xi(x) = c_1 e^{-\frac{x}{\sqrt{\mu}}} + c_2 e^{\frac{x}{\sqrt{\mu}}}, \tag{A2}$$

and thus

$$v_s(x) = \mu c_1 e^{-\frac{x}{\sqrt{\mu}}} + \mu c_2 e^{\frac{x}{\sqrt{\mu}}} + \frac{\gamma}{2}x^2 + c_3 x + c_4. \tag{A3}$$

Using simply supported boundary conditions and applying simplifications, the static solution can be obtained as

$$\begin{aligned} v_s(x) = &-\gamma\mu \operatorname{sech}\left(\frac{1}{2\sqrt{\mu}}\right)\cosh\left(\frac{1-2x}{2\sqrt{\mu}}\right) \\ &+ \frac{\gamma}{2}(x^2 - x + 2\mu). \end{aligned} \tag{A4}$$

Appendix B

In this appendix, we present the proof of the convergence of the series for C_k (see (29)), where k is a fixed, even integer. Consider the series sum:

$$\begin{aligned} C_k = &\sum_{j=0}^{\infty} \frac{1}{2j+1} \int_0^1 U' \sin((2j+1)\pi x)\sin(k\pi x)dx \\ = &\, S_1 - S_2, \end{aligned} \tag{B5}$$

where

$$\begin{aligned} S_1 := &\sum_{j=0}^{\infty} \frac{4\gamma k\mu\pi^2}{(1+(2j+1-k)^2\mu\pi^2)(1+(2j+1+k)^2\mu\pi^2)} \\ S_2 := &\sum_{j=0}^{\infty} \frac{4\gamma k}{\mu\pi^2(2j+1-k)^2(2j+1+k)^2}. \end{aligned} \tag{B6}$$

Convergence of S_1

To prove the convergence of S_1, we start by proving the convergence of the series sum over the index set $\mathbb{N} \setminus \{k\}$:

$$\widetilde{S}_1 := \sum_{i=0}^{k-1} a_i + \sum_{i=k+1}^{\infty} a_i, \tag{B7}$$

where

$$a_i = \frac{4\gamma k\mu\pi^2}{(1+(i-k)^2\mu\pi^2)(1+(i+k)^2\mu\pi^2)}. \tag{B8}$$

The series $\sum_{i=0}^{k-1} a_i$ is finite and hence bounded. For $i \geq k+1$, let $n = i + k$. Then:

$$\sum_{i=k+1}^{\infty} a_i = \sum_{n=1}^{\infty} \frac{4\gamma k\mu\pi^2}{(1+n^2\mu\pi^2)(1+(n+2k)^2\mu\pi^2)}. \tag{B9}$$

Bounding the series:

$$\begin{aligned}|\sum_{i=k+1}^{\infty} a_i| &\leq \sum_{i=k+1}^{\infty} |a_i| < \sum_{n=1}^{\infty} \frac{4\gamma k\mu\pi^2}{(1+n^2\mu\pi^2)^2} \\ &< \sum_{n=1}^{\infty} \frac{4\gamma k}{\mu\pi^2 n^4} = \frac{4\gamma k}{\mu\pi^2} \sum_{n=1}^{\infty} \frac{1}{n^4} = \frac{2\gamma k\pi^2}{45\mu}.\end{aligned} \tag{B10}$$

This concludes that $\widetilde{S}_1$ is absolutely convergent, implying S_1 is also convergent.

Convergence of S_2

To prove the convergence of S_2, we define a series sum $\widetilde{S}_2$, on the index set of natural numbers with $i \neq k$:

$$\widetilde{S}_2 = \sum_{i=0}^{k-1} b_i + \sum_{i=k+1}^{\infty} b_i, \tag{B11}$$

where

$$b_i = \frac{4\gamma k}{\mu\pi^2(i-k)^2(i+k)^2}. \tag{B12}$$

The series $\sum_{i=0}^{k-1} a_i$ is finite and hence bounded. For $i \geq k+1$, let $n = i+k$. Then:

$$\sum_{i=k+1}^{\infty} b_i = \sum_{n=1}^{\infty} \frac{4\gamma k}{\mu\pi^2 n^2(n+2k)^2}. \tag{B13}$$

Bounding the series:

$$\begin{aligned}|\sum_{i=k+1}^{\infty} b_n| &\leq \sum_{i=k+1}^{\infty} |b_n| < \sum_{n=1}^{\infty} \frac{4\gamma k}{\mu\pi^2 n^4} \\ &< \sum_{n=1}^{\infty} \frac{4\gamma k}{\mu\pi^2 n^4} = \frac{4\gamma k}{\mu\pi^2} \sum_{n=1}^{\infty} \frac{1}{n^4} = \frac{2\gamma k\pi^2}{45\mu}.\end{aligned} \tag{B14}$$

This shows that $\widetilde{S}_2$ is absolutely convergent, implying that S_2 is convergent.

Since both S_1 and S_2 are convergent, their difference $C_k = S_1 - S_2$ is also convergent, hence C_k is a constant.

Appendix C

In this appendix, the intermediate steps of simplifications between system (49) and system (50) are given.

System (49) is given by

$$\begin{aligned}\dot{A}_K &= -aA_K + p\sin(\varphi t_1)A_N + p\cos(\varphi t_1)B_N, \\ \dot{B}_K &= -aB_K - p\cos(\varphi t_1)A_N + p\sin(\varphi t_1)B_N, \\ \dot{A}_N &= -bA_N - q\sin(\varphi t_1)A_K + q\cos(\varphi t_1)B_K, \\ \dot{B}_N &= -bB_N - q\cos(\varphi t_1)A_K - q\sin(\varphi t_1)B_K.\end{aligned} \tag{C15}$$

By differentiating the first equation in (C15), it follows that

$$\begin{aligned}\ddot{A}_K &= -a\dot{A}_K + p\sin(\varphi t_1)\dot{A}_N + p\cos(\varphi t_1)\dot{B}_N \\ &\quad + p\varphi[\cos(\varphi t_1)A_N - \sin(\varphi t_1)B_N] \\ &= -a\dot{A}_K - bp\sin(\varphi t_1)A_N - bp\cos(\varphi t_1)B_N \\ &\quad - pqA_K - \varphi(\dot{B}_K + aB_K) \\ &= -(a+b)\dot{A}_K - (ab+pq)A_K \\ &\quad - \varphi(\dot{B}_K + aB_K).\end{aligned} \tag{C16}$$

Using the same approach, we can also find

$$\begin{aligned}\ddot{B}_K &= -(a+b)\dot{B}_K - (ab+pq)B_K \\ &\quad + \varphi(\dot{A}_K + aA_K).\end{aligned} \tag{C17}$$

Appendix D

In this appendix, the intermediate steps to derive of system (94) from system (93) are presented. Consider system (93): a

$$\begin{aligned}\dot{A}_K &= -aA_K + r[\sin(\varphi t_1)A_N + \cos(\varphi t_1)B_N], \\ \dot{B}_K &= -aB_K - r[\cos(\varphi t_1)A_N - \sin(\varphi t_1)B_N], \\ \dot{A}_N &= -bA_N - s[\sin(\varphi t_1)A_K - \cos(\varphi t_1)B_K] \\ &\quad - p[\sin(\varphi t_1)A_L - \cos(\varphi t_1)B_L],\end{aligned} \tag{D18a}$$

$$\begin{aligned}\dot{B}_N &= -bB_N - s[\cos(\varphi t_1)A_K + \sin(\varphi t_1)B_K] \\ &\quad + p[\cos(\varphi t_1)A_L + \sin(\varphi t_1)B_L], \\ \dot{A}_L &= -cA_L - q[\sin(\varphi t_1)A_K - \cos(\varphi t_1)B_K], \\ \dot{B}_L &= -cB_L + q[\cos(\varphi t_1)A_K + \sin(\varphi t_1)B_K].\end{aligned} \tag{D18b}$$

By differentiating the third equation in system (D18), it follows that

$$\begin{aligned}\ddot{A}_N &= -b\dot{A}_N - s[\sin(\varphi t_1)\dot{A}_K - \cos(\varphi t_1)\dot{B}_K] \\ &\quad - p[\sin(\varphi t_1)\dot{A}_L - \cos(\varphi t_1)\dot{B}_L] \\ &\quad - \varphi\big\{s[\cos(\varphi t_1)A_K + \sin(\varphi t_1)B_K] \\ &\quad + p[\cos(\varphi t_1)A_L + \sin(\varphi t_1)B_L]\big\} \qquad \text{(D19)}\\ &= -b\dot{A}_N - (rs - pq)A_N \\ &\quad + as[\sin(\varphi t_1)A_K - \cos(\varphi t_1)B_K] \\ &\quad + cp[\sin(\varphi t_1)A_L - \cos(\varphi t_1)B_L] \qquad \text{(D20)}\\ &\quad - \varphi\big\{s[\cos(\varphi t_1)A_K + \sin(\varphi t_1)B_K] \\ &\quad + p[\cos(\varphi t_1)A_L + \sin(\varphi t_1)B_L]\big\},\end{aligned}$$

and by differentiating Eq. (D20) once again it follows that

$$\begin{aligned}\dddot{A}_N &= -b\ddot{A}_N - (rs - pq)\dot{A}_N \\ &\quad - a^2 s[\sin(\varphi t_1)A_K - \cos(\varphi t_1)B_K] \\ &\quad - c^2 p[\sin(\varphi t_1)A_L - \cos(\varphi t_1)B_L] \\ &\quad + \varphi^2[\dot{A}_N + bA_N] + \varphi\Big\{(rs + pq)B_N \qquad \text{(D21)}\\ &\quad - 2as[\cos(\varphi t_1)A_K + \sin(\varphi t_1)B_K] \\ &\quad - 2cp[\cos(\varphi t_1)A_L + \sin(\varphi t_1)B_L]\Big\}.\end{aligned}$$

We know that, for $\varphi = 0$, the detuned system has to be equivalent with the pure resonance system (90). Therefore, we can infer the necessary further manipulations by comparing the characteristic polynomial (90) with the characteristic polynomials of the equations (D21) and its analogous equation for $\dddot{B}_N$ when $\varphi = 0$. By doing so, we can observe that the missing terms are:

$$\begin{aligned}&- (a + c)[\ddot{A}_N + bA_N + (rs - pq)A_N] \\ &\quad - ac[\dot{A}_N + bA_N] \\ &\quad = -(a + c)\Big\{as[\sin(\varphi t_1)A_K - \cos(\varphi t_1)B_K] \\ &\qquad + cp[\sin(\varphi t_1)A_L - \cos(\varphi t_1)B_L] \\ &\qquad - \varphi s[\cos(\varphi t_1)A_K + \sin(\varphi t_1)B_K] \\ &\qquad - \varphi p[\cos(\varphi t_1)A_L + \sin(\varphi t_1)B_L]\Big\} \\ &\quad + ac\Big\{s[\sin(\varphi t_1)A_K - \cos(\varphi t_1)B_K] \\ &\qquad + p[\sin(\varphi t_1)A_L - \cos(\varphi t_1)B_L]\Big\}. \qquad \text{(D22)}\end{aligned}$$

Knowing

$$\begin{aligned}&- a^2 s[\sin(\varphi t_1)A_K - \cos(\varphi t_1)B_K] \\ &\quad - c^2 p[\sin(\varphi t_1)A_L - \cos(\varphi t_1)B_L] \\ &\quad = -(a + c)[\ddot{A}_N + bA_N + (rs - pq)A_N] \\ &\qquad - ac[\dot{A}_N + bA_N] \\ &\qquad - \Big\{as[\cos(\varphi t_1)A_K + \sin(\varphi t_1)B_K] \\ &\qquad + ap[\sin(\varphi t_1)A_L + \cos(\varphi t_1)B_L] \\ &\qquad + cs[\cos(\varphi t_1)A_K + \sin(\varphi t_1)B_K] \\ &\qquad + cp[\cos(\varphi t_1)A_L + \sin(\varphi t_1)B_L]\Big\}, \qquad \text{(D23)}\end{aligned}$$

we can obtain

$$\begin{aligned}\dddot{A}_N &= -(a + b + c)\ddot{A}_N \\ &\quad - (ab + bc + ac + rs - pq)\dot{A}_N \\ &\quad - (abc - apq + crs)A_N \\ &\quad - \varphi[(ab - bc + rs + pq)B_N + (a - c)\dot{B}_N] \\ &\quad - \varphi^2[\dot{A}_N + bA_N]. \qquad \text{(D24)}\end{aligned}$$

The same steps can be followed for the fourth equation in (D18) to find

$$\begin{aligned}\dddot{B}_N &= -(a + b + c)\ddot{B}_N \\ &\quad - (ab + bc + ac + rs - pq)\dot{B}_N \\ &\quad - (abc - apq + crs)B_N \\ &\quad + \varphi[(ab - bc + rs + pq)A_N + (a - c)\dot{A}_N] \\ &\quad - \varphi^2[\dot{B}_N + bB_N]. \qquad \text{(D25)}\end{aligned}$$

Appendix E

In this appendix, the coefficients of the characteristic polynomial (96) and the determinants in the Routh-Hurwitz criterion are provided. Considering the case $\Omega = \omega_3 - \omega_2 + \varepsilon\varphi = \omega_2 + \omega_1 + \varepsilon\varphi$ for $\mu \gg 1$, the coefficients of the characteristic polynomial (96) corresponding to Eq. (94) with the parameter values (95) are a

$$d_6 = 1, \quad d_5 = 98\alpha\pi^4,$$

$$
\begin{aligned}
d_4 &= \frac{6195\alpha^2\pi^8}{2} + \frac{288(\sqrt{\beta}V_1)^2}{25} + 2\varphi^2\\
d_3 &= \frac{68905}{2}\alpha^3\pi^{12} + \frac{12256}{25}\alpha\pi^4(\sqrt{\beta}V_1)^2\\
&\quad + 114\alpha\pi^4\varphi^2\\
d_2 &= \varphi^4 + \left(\frac{288(\sqrt{\beta}V_1)^2}{25} + \frac{6161\alpha^2\pi^8}{2}\right)\varphi^2\\
&\quad + \frac{2194465\alpha^4\pi^{16}}{16} + \frac{20736(\sqrt{\beta}V_1)^4}{625}\\
&\quad + \frac{9352\alpha^2(\sqrt{\beta}V_1)^2\pi^8}{25}\\
d_1 &= 16\alpha\varphi^4\pi^4\\
&\quad + \left(\frac{15968}{25}\alpha\pi^4(\sqrt{\beta}V_1)^2 + 31496\alpha^3\pi^{12}\right)\varphi^2\\
&\quad + 112833\alpha^5\pi^{20} - \frac{599696\alpha^3(\sqrt{\beta}V_1)^2\pi^{12}}{25}\\
&\quad - \frac{267264\alpha(\sqrt{\beta}V_1)^4\pi^4}{625}\\
d_0 &= 64\alpha^2\varphi^4\pi^8 + \Bigg[104992\alpha^4\pi^{16}\\
&\quad + \frac{37636}{625}(\sqrt{\beta}V_1)^4\\
&\quad + \frac{109312}{25}\alpha^2(\sqrt{\beta}V_1)^2\pi^8\Bigg]\varphi^2\\
&\quad - \frac{300672\alpha^4(\sqrt{\beta}V_1)^2\pi^{16}}{25}\\
&\quad + \frac{861184\alpha^2(\sqrt{\beta}V_1)^4\pi^8}{625}\\
&\quad + 26244\alpha^6\pi^{24}
\end{aligned}
\tag{E26}
$$

The Routh-Hurwitz stability criterion is satisfied for a sixth order system by $T_i > 0, i = 0, 1, \ldots, 6$ where T_i are defined as

$$
\begin{aligned}
&T_0 = d_6, \quad T_1 = d_5, \quad T_2 = \det\begin{pmatrix} d_5 & d_6\\ d_3 & d_4\end{pmatrix},\\
&T_3 = \det\begin{pmatrix} d_5 & d_6 & 0\\ d_3 & d_4 & d_5\\ d_1 & d_2 & d_3\end{pmatrix},\\
&T_4 = \det\begin{pmatrix} d_5 & d_6 & 0 & 0\\ d_3 & d_4 & d_5 & d_6\\ d_1 & d_2 & d_3 & d_4\\ 0 & d_0 & d_1 & d_2\end{pmatrix},
\end{aligned}
\tag{E27a}
$$

$$
\begin{aligned}
T_5 &= \det\begin{pmatrix} d_5 & d_6 & 0 & 0 & 0\\ d_3 & d_4 & d_5 & d_6 & 0\\ d_1 & d_2 & d_3 & d_4 & d_5\\ 0 & d_0 & d_1 & d_2 & d_3\\ 0 & 0 & 0 & d_0 & d_1\end{pmatrix},\\
T_6 &= \det\begin{pmatrix} d_5 & d_6 & 0 & 0 & 0 & 0\\ d_3 & d_4 & d_5 & d_6 & 0 & 0\\ d_1 & d_2 & d_3 & d_4 & d_5 & d_6\\ 0 & d_0 & d_1 & d_2 & d_3 & d_4\\ 0 & 0 & 0 & d_0 & d_1 & d_2\\ 0 & 0 & 0 & 0 & 0 & d_0\end{pmatrix}.
\end{aligned}
\tag{E27b}
$$

Substituting the coefficients $d_0, \ldots, d_6$ obtained in (E26) into (E27), leads to seven algebraic equations in $(\varphi, \alpha, \sqrt{\beta}V_1)$. The stability domain for the fixed detuning parameter φ is defined as $\mathcal{S} := \{(\alpha, \sqrt{\beta}V_1)| \cap_{i=0}^{6} (T_i^{\varphi}(\alpha, \sqrt{\beta}V_1) > 0)\}$.

Appendix F

In this appendix, we outline the Crank-Nicolson type scheme used to solve the PDE in Eq. (9), with boundary conditions in Eq. (10) and initial conditions in Eq. (11). The following finite difference operators approximate the partial derivatives, where Δt and Δx are the time and space step sizes, and $\delta_t^{(p)}$ and $\delta_x^{(q)}$ are the p-th and q-th order partial difference operators, respectively:

$$
\begin{aligned}
[\delta_x^4 u]_k^n &= \frac{u_{k+2}^n - 4u_{k+1}^n + 6u_k^n - 4u_{k-1}^n + u_{k-2}^n}{(\Delta x)^4},\\
[\delta_x^2 u]_k^n &= \frac{u_{k+1}^n - 2u_k^n + u_{k-1}^n}{(\Delta x)^2},\\
[\delta_x u]_k^n &= \frac{u_{k+1}^n - u_{k-1}^n}{2\Delta x},\\
[\delta_t^2 u]_k^n &= \frac{u_k^{n+1} - 2u_k^n + u_k^{n-1}}{(\Delta t)^2},\\
[\delta_t u]_k^n &= \frac{u_k^{n+1} - u_k^{n-1}}{2\Delta t},
\end{aligned}
\tag{F28}
$$

All of the operators used here are second-order accurate.

Also knowing that $t^n = n\Delta t$, we can write fluid velocity and its derivative, $V^{(n)} = \varepsilon(V_0 +$

$V_1 \sin(\Omega n \Delta t))$ and $V_t^{(n)} = \varepsilon \Omega V_1 \cos(\Omega n \Delta t)$

$$
\begin{aligned}
A :=& I + \Delta t^2 \Bigg(\frac{\mu}{3} [\delta_x^4]_k^{n+1} + \frac{\varepsilon\alpha}{2\Delta t} [\delta_x^4]_k^{n+1} - \frac{1}{3} [\delta_x^2]_k^{n+1} \\
&+ \frac{2\sqrt{\beta} V^{(n+1)}}{2\Delta t} [\delta_x u]_k^{n+1} + (V^{(n+1)})^2 [\delta_x^2]_k^{n+1} \\
&+ \sqrt{\beta} V_t^{(n)} [\delta_x u]_k^{n+1} \Bigg) \\
B :=& 2I + \Delta t^2 (-\frac{\mu}{3} [\delta_x^4]_k^n + \frac{1}{3} [\delta_x^2]_k^n) \\
C :=& -I + \Delta t^2 \Bigg(-\frac{\mu}{3} [\delta_x^4]_k^{n-1} + \varepsilon\alpha [\delta_x^4]_k^{n-1} \\
&+ \frac{1}{3} [\delta_x^2]_k^{n-1} + \frac{2\sqrt{\beta} V^{(n+1)}}{2\Delta t} [\delta_x u]_k^{n-1} \Bigg)
\end{aligned}
\tag{F29}
$$

and knowing $\boldsymbol{u}^n$ and $\boldsymbol{u}^{n-1}$, $\boldsymbol{u}^{n+1}$ can be solved from

$$
A\boldsymbol{u}^{n+1} = B\boldsymbol{u}^n + C\boldsymbol{u}^{n-1} - \gamma \tag{F30}
$$

using a preferred linear solver method.

References

1. Bourriéres, F.-J.: Sur un phénomène d'oscillation auto-entretenue en mécanique des fluides réels. (1939)
2. Ashley, H., Haviland, G.: Bending vibrations of a pipe line containing flowing fluid. J. Appl. Mech. **17**(3), 229–232 (1950)
3. Housner, G.W.: Bending vibrations of a pipe line containing flowing fluid. J. Appl. Mech. **19**(2), 205–208 (1952)
4. Benjamin, T.B.: Dynamics of a system of articulated pipes conveying fluid - I. Theory. Proc. R. Soc. Lond. A **261**(1307), 457–486 (1961)
5. Paidoussis, M.P., Issid, N.T.: Dynamic stability of pipes conveying fluid. J. Sound Vib. **33**(3), 267–294 (1974)
6. Paidoussis, M.P., Laithier, B.E.: Dynamics of timoshenko beams conveying fluid. J. Mech. Eng. Sci. **18**(4), 210–220 (1976)
7. Semler, C., Li, G.X., Paidoussis, M.P.: The non-linear equations of motion of pipes conveying fluid. J. Sound Vib. **169**(5), 577–599 (1994)
8. Chen, S.-S.: Dynamic stability of tube conveying fluid. J .Eng. Mech. Div. **97**(5), 1469–1485 (1971)
9. Bohn, M.P., Herrmann, G.: The dynamic behavior of articulated pipes conveying fluid with periodic flow rate. J. Appl. Mech. **41**(1), 55–62 (1974)
10. Paidoussis, M.P., Sundararajan, C.: Parametric and combination resonances of a pipe conveying pulsating fluid. J. Appl. Mech. **42**(4), 780–784 (1975)
11. Ariaratnam, S.T., Sri Namachchivaya, N.: Dynamic stability of pipes conveying pulsating fluid. J. Sound Vib. **107**(2), 215–230 (1986)
12. Sri Namchchivaya, N.: Non-linear dynamics of supported pipe conveying pulsating fluid-I. Subharmonic resonance. Int. J. Non-Linear Mech. **24**(3), 185–196 (1989)
13. Sri Namchchivaya, N., Tien, W.M.: Non-linear dynamics of supported pipe conveying pulsating fluid-II. Combination resonance. Int. J. Non-Linear Mech. **24**(3), 197–208 (1989)
14. Semler, C., Paidoussis, M.P.: Nonlinear analysis of the parametric resonances of a planar fluid-conveying cantilevered pipe. J. Fluids Struct. **10**(7), 787–825 (1996)
15. Öz, H.R., Boyaci, H.: Transverse vibrations of tensioned pipes conveying fluid with time-dependent velocity. J. Sound Vib. **236**(2), 259–276 (2000)
16. Jin, J.D., Song, Z.Y.: Parametric resonances of supported pipes conveying pulsating fluid. J. Fluids Struct. **20**(6), 763–783 (2005)
17. Panda, L.N., Kar, R.C.: Nonlinear dynamics of a pipe conveying pulsating fluid with parametric and internal resonances. Nonlinear Dyn. **49**(1), 9–30 (2007)
18. Panda, L.N., Kar, R.C.: Nonlinear dynamics of a pipe conveying pulsating fluid with combination, principal parametric and internal resonances. J. Sound Vib. **309**(3), 375–406 (2008)
19. Luongo, A., Zulli, D., Piccardo, G.: Analytical and numerical approaches to nonlinear galloping of internally resonant suspended cables. J. Sound Vib. **315**(3), 375–393 (2008). https://doi.org/10.1016/j.jsv.2008.03.067
20. Di Nino, S., Luongo, A.: Nonlinear interaction between self- and parametrically excited wind-induced vibrations. Nonlinear Dyn. **103**(1), 79–101 (2021). https://doi.org/10.1007/s11071-020-06114-3
21. Wang, L., Jiang, T.L., Dai, H.L., Ni, Q.: Three-dimensional vortex-induced vibrations of supported pipes conveying fluid based on wake oscillator models. J. Sound Vib. **422**, 590–612 (2018). https://doi.org/10.1016/j.jsv.2018.02.032
22. Zhu, B., Zhang, X., Zhao, T.: Nonlinear planar and non-planar vibrations of viscoelastic fluid-conveying pipes with external and internal resonances. J. Sound Vib. **548**, 117558 (2023). https://doi.org/10.1016/j.jsv.2023.117558
23. Jin, Q., Yuan, F.-G., Ren, Y.: Resonance interaction of flow-conveying nanotubes under forced vibration. Acta Mech. **234**(6), 2497–2517 (2023). https://doi.org/10.1007/s00707-022-03425-x
24. Dou, B., Ding, H., Mao, X., Wei, S., Chen, L.: Dynamic modeling of fluid-conveying pipes restrained by a retaining clip. Appl. Math. Mech. **44**(8), 1225–1240 (2023). https://doi.org/10.1007/s10483-023-3016-9
25. Mao, X.-Y., Jing, J., Ding, H., Chen, L.-Q.: Dynamics of axially functionally graded pipes conveying fluid. Nonlinear Dyn. **111**(12), 11023–11044 (2023). https://doi.org/10.1007/s11071-023-08470-2
26. Wei, S., Yan, X., Li, X., Ding, H., Chen, L.-Q.: Parametric vibration of a nonlinearly supported pipe conveying pulsating fluid. Nonlinear Dyn. **111**(18), 16643–16661 (2023). https://doi.org/10.1007/s11071-023-08761-8
27. Deng, T.-C., Ding, H., Mao, X.-Y., Chen, L.-Q.: Natural vibration of pipes conveying high-velocity fluids with multiple distributed retaining clips. Nonlinear Dyn. **111**(20), 18819–18836 (2023). https://doi.org/10.1007/s11071-023-08807-x
28. Mao, X.-Y., Shu, S., Fan, X., Ding, H., Chen, L.-Q.: An approximate method for pipes conveying fluid with strong

boundaries. J. Sound Vib. **505**, 116157 (2021). https://doi.org/10.1016/j.jsv.2021.116157
29. Lu, Z.-Q., Zhang, K.-K., Ding, H., Chen, L.-Q.: Internal resonance and stress distribution of pipes conveying fluid in supercritical regime. Int. J. Mech. Sci. **186**, 105900 (2020). https://doi.org/10.1016/j.ijmecsci.2020.105900
30. Suweken, G., van Horssen, W.T.: On the transversal vibrations of a conveyor belt with a low and time-varying velocity. Part I: the string-like case. J. Sound Vib. **264**(1), 117–133 (2003)
31. Suweken, G., van Horssen, W.T.: On the transversal vibrations of a conveyor belt with a low and time-varying velocity. Part II: the beam-like case. J. Sound Vib. **267**(5), 1007–1027 (2003)
32. Suweken, G., van Horssen, W.T.: On the weakly nonlinear, transversal vibrations of a conveyor belt with a low and time-varying velocity. Nonlinear Dyn. **31**(2), 197–223 (2003)
33. Pakdemirli, M., Öz, H.R.: Infinite mode analysis and truncation to resonant modes of axially accelerated beam vibrations. J. Sound Vib. **311**(3), 1052–1074 (2008)
34. van Horssen, W.T.: On the influence of lateral vibrations of supports for an axially moving string. J. Sound Vib. **268**(2), 323–330 (2003)
35. van Horssen, W.T., Ponomareva, S.V.: On the construction of the solution of an equation describing an axially moving string. J. Sound Vib. **287**(1), 359–366 (2005)
36. Ponomareva, S.V., van Horssen, W.T.: On transversal vibrations of an axially moving string with a time-varying velocity. Nonlinear Dyn. **50**(1), 315–323 (2007)
37. Malookani, R.A., van Horssen, W.T.: On resonances and the applicability of Galerkin's truncation method for an axially moving string with time-varying velocity. J. Sound Vib. **344**, 1–17 (2015)
38. Malookani, R.A., Van Horssen, W.T.: On the vibrations of an axially moving string with a time-dependent velocity. In: Volume 4B: Dynamics, Vibration, and Control, pp. 04–04061. American Society of Mechanical Engineers, Houston, Texas, USA (2015). https://doi.org/10.1115/IMECE2015-50452
39. Sandilo, S.H., van Horssen, W.T.: On variable length induced vibrations of a vertical string. J. Sound Vib. **333**(11), 2432–2449 (2014)
40. Malookani, R.A., van Horssen, W.T.: On parametric stability of a nonconstant axially moving string near resonances. J. Vib. Acoust. **139**, 011005 (2016)
41. Malookani, R.A., van Horssen, W.T.: On the asymptotic approximation of the solution of an equation for a non-constant axially moving string. J. Sound Vib. **367**, 203–218 (2016)
42. Andrianov, I.V., van Horssen, W.T.: On the transversal vibrations of a conveyor belt: applicability of simplified models. J. Sound Vib. **313**(3), 822–829 (2008)
43. Ponomareva, S.V., van Horssen, W.T.: On the transversal vibrations of an axially moving continuum with a time-varying velocity: transient from string to beam behavior. J. Sound Vib. **325**(4), 959–973 (2009)
44. Ponomareva, S., van Horssen, W.T.: On applying the Laplace transform method to an equation describing an axially moving string. PAMM **4**(1), 107–108 (2004)